ADVANCES IN INORGANIC CHEMISTRY, VOL. 40

# COMPLEXES OF STERICALLY HINDERED THIOLATE LIGANDS

J. R. DILWORTH and J. HU

Department of Chemistry and Biological Chemistry, University of Essex, Colchester, Essex CO4 3SQ, England



## I. Aim and Scope

There have been extensive studies of thiolate complexes due to their possible relevance to the structure, bonding, and function of biologically active reaction centers in metalloproteins such as ferredoxins, nitrogenases, blue copper proteins, and metallothioneins. There is a rich coordination chemistry and a remarkable diversity of structural types in this area, and the topic has been the subject of several reviews (*1–5*). One particular aspect of this chemistry that has been expanding rapidly is the deployment of sterically hindered thiolate ligands, and recent work has demonstrated that such ligands afford complexes with unusual geometries and oxidation states and low coordination numbers. Their complexes frequently have enhanced solubilities, and some of them are capable of binding small substrate molecules due to their

formal coordinative unsaturation. Moreover, the steric requirements of the ligands favor the formation of mononuclear complexes rather than the thiolate bridged oligomers usually generated by using sterically unencumbered thiols.

The chemistry of sterically hindered thiolate complexes as a whole has not been reviewed previously, although they have been included in the earlier more general reviews of the chemistry of thiolate and other sulfur ligands (*1, 2*). This survey covers the chemistry of transition metal and main group complexes of sterically hindered thiolates up to the end of 1991. Emphasis is placed on their syntheses, structural types, and reactivity, and spectroscopic studies have generally been omitted. Generally only those complexes that contain at least 50% of sterically hindered thiolate ligands in the coordination sphere are considered in this chapter on the basis that a lower proportion would not be sufficient to dominate the coordination chemistry. The account covers 2,6- and 2,4,6-alkyl and silyl-substituted aromatic thiolate complexes in reasonable depth. However, halogenated aromatic thiolate and sterically hindered aliphatic thiolate complexes are mentioned where appropriate. The recent development of sterically hindered multidentate thiolate complexes has revealed much intriguing chemistry, but we have decided to omit these as chelate rather than steric effects predominate. The chapter is therefore primarily focused on monodentate thiolate ligands.

## II. Structures and Syntheses of Sterically Hindered Thiols

The structures and abbreviations for the most commonly used bulky 2,6- and 2,4,6-substituted aromatic thiols are shown in Fig. 1. These aromatic thiols have the advantage over those with aliphatic groups that the tendency for C—S bond cleavage is virtually eliminated, which in turn lessens the probability of generating unreactive sulfide-bridged polymers.

The synthesis of these thiols is relatively straightforward from commercially available phenols via the Newman–Karnes rearrangement (*6*) (Eq. (1)) or from sulfonyl chlorides (also obtainable commercially) by $Li[AlH_4]$ reduction (*7*) (Eq. (2)).

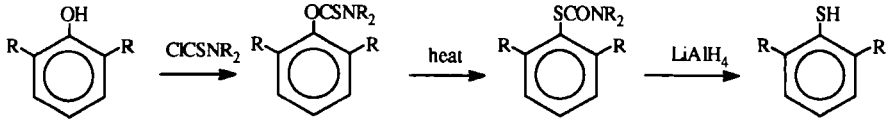


(1)

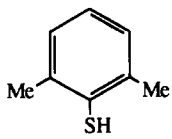


DMTH

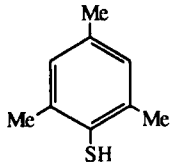


TMTH

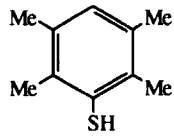


TEMTH

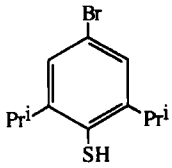


DIPBTH

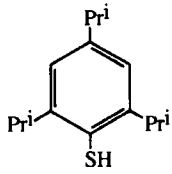


TIPTH

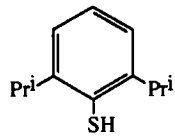


DIPTH

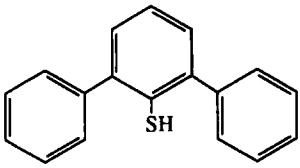


DPTH


PFTPH

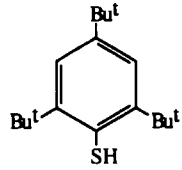


TBTPH

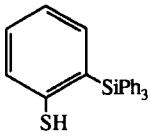


TPSTPH


STPH

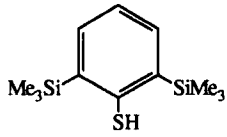


BSTPH

FIG. 1.

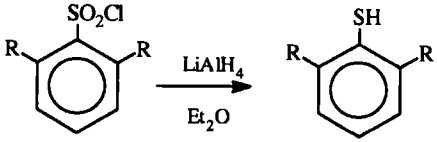


(2)

Recently the range of sterically demanding aromatic thiols has been expanded by the introduction of a comparatively simple high-yield synthetic route to 2,6-diorganosilylthiophenols via the lithiation of thiophenol (*8, 9*) (Eq.(3)). An attractive feature of this class of ligand

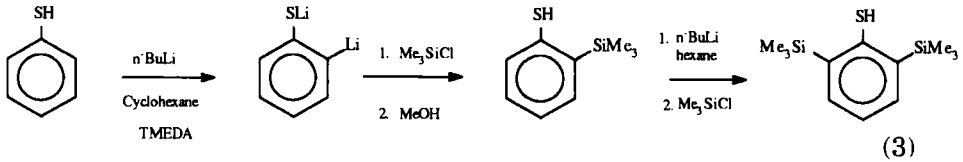


(3)

is that the steric and electronic demands of the ligands can be varied at will by employing a range of organosilyl groups. The coordination chemistry of this type of ligand remains comparatively unexplored. The presence of alkyl or organosilyl substituents in the aromatic ring greatly increases the solubility of the complexes in hydrocarbon solvents, sometimes to the extent that the complexes can be obtained as solids only with great difficulty. Fortunately such complexes are frequently relatively insoluble in polar solvents such as methanol or acetonitrile.

An alternative route using tetrahydropyran (THP) (Eq. (4)) as a protecting group for sulfur is less convenient, but also proceeds in good overall yields (*10, 11*). An interesting variation of the route detailed in Eq. (3) is that potentially coordinating substituents such as $Ph_2P$ can be introduced at the 2-position, giving rise to a range of powerful bi- and polydentate chelating ligands. Addition of the phosphorus group at the stage of the second lithiation provides access to a range of bulky P—S donors that have novel coordination chemistry. Unfortunately the latter class of ligand lies outside the scope of this review.

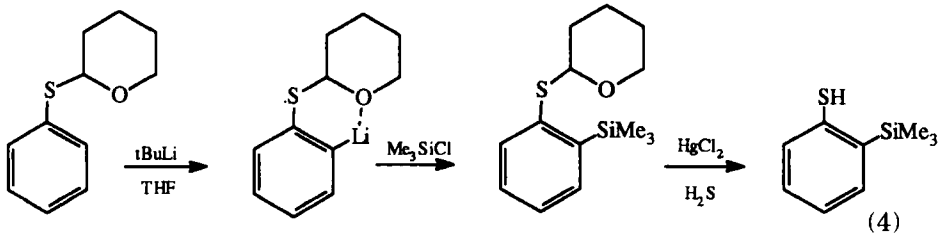


(4)

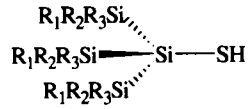


$R_1$, $R_2$, $R_3$ = alkyl or aryl

FIG. 2.

The polyorganosilylmethyl thiolates of the type shown in Fig. 2 have been made by a variety of routes, of which the most convenient is probably the silylation of $THPSCH_2Li$, followed by metallation and silylation sequences until the requisite number of organosilyl groups have been introduced (*8, 10*). Tris(trimethylsily)methanethiol expels a trimethylsilyl group upon heating, and this provides alternative access to bis(trimethylsilyl)methanethiol. The coordination chemistry of such ligands has been very little studied, partly as the ligand synthesis is time consuming and also due to the very high solubility of the complexes, which often thwarts their separation. Indeed the only systematic study of their chemistry has been with Ag(I), where the polymeric nature of the complexes facilitates their separation.

## III. Transition Metal Complexes

### A. Titanium, Zirconium, Hafnium, Vanadium, Niobium, and Tantalum

There are surprisingly few reported thiolate complexes of the early transition metals, although there is no a priori reason why thiolates should not bind well to such metals. The first to be reported were the neutral M(IV) complexes $[M(TMT)_4]$ (M = Ti,Zr), and these are almost certainly mononuclear and tetrahedral (*12*). The anionic homoleptic $d^1$ titanium(III) thiolate complex $[Ti(TIPT)_4]^-$ was prepared by the reaction of $TiCl_3$ with the lithium salt of TIPT in diethyl ether (*13*). The X-ray crystal structure revealed that the complex has distorted-tetrahedral coordination about the metal with the thiolate ligands orientated so as to minimize steric repulsion. The distortion toward $D_{2d}$ symmetry by a flattening of the tetrahedral geometry was thought to be due either to crystal packing forces or a nondegenerate ground state. A similar distortion of tetrahedral geometry has been reported for

$[Mo(TIPT)_4]$ (*14*). In comparison with the analogous phenoxide complex $[Ti(OC_6H_4\text{-}2,6\text{-}Pr_2^i)_4]$ (*15*), the large difference in the Ti—S—C (110°) and Ti—O—C (150°) bond angles was attributed to greater oxygen–metal $p$–$d$ $\pi$ overlap.

The complex $[Ti(SBu^t)_4]$ has been obtained from the reaction of $[Ti(NMe_2)_4]$ with $Bu^tSH$. It is appreciably volatile, and low-pressure vapor-phase thermolysis gave pure X-ray amorphous TiS (*15a*). An intriguing series of complex zirconium clusters with various combinations of bridging sulfide and thiolate ligands have been obtained by the reaction of labile Zr(IV) precursors with $Bu^tSH$. Thus reaction of $[Zr(CH_2Ph)_4]$ with four equivalents of $Bu^tSH$ in toluene gave a high yield of the cluster $[Zr_3(\mu_3\text{-}S)(SBu^t)_{10}]$. An X-ray crystal structure (Fig. 3) revealed a $Zr_3(\mu\text{-}SBu^t)_3$ core with capping triply bridging S and $SBu^t$ ligands and approximately hexagonal bipyramidal geometry (*15b*). The Zr—S bond distance of 2.765(5) Å for the triply bridging $Bu^tS$ ligands is longer than the sum of the covalent radii for Zr and S, and it was suggested that this ligand should be correspondingly labile. The reaction of $[Zr(BH_4)_4]$ with $Bu^tSH$ in THF gave an even more complex cluster $[Zr_3S_2(SBu^t)_2(BH_4)_4(THF)_2]$, which was shown by an X-ray crystal structure to have a $Zr_3(\mu_3\text{-}S)(\mu\text{-}SBu^t)_2(\mu\text{-}S)$ core. Two Zr atoms have

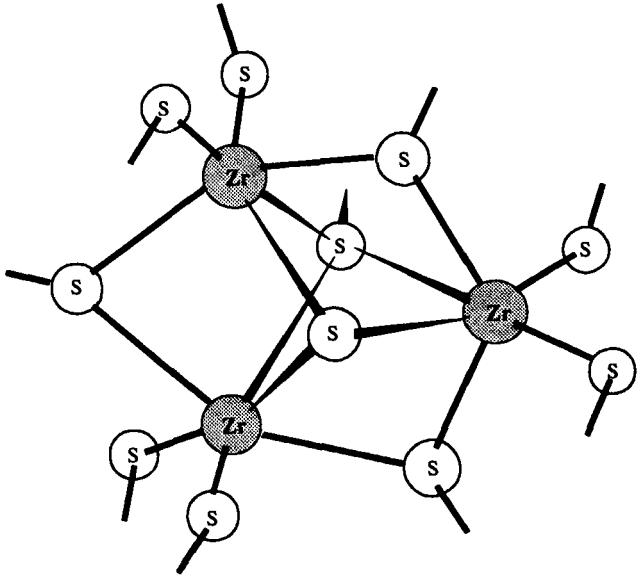


FIG. 3.

terminal triply bridging $BH_4$ and THF ligands and the other two $BH_4$ ligands, one triply and the other doubly bridging (*15c*).

The mononuclear homoleptic vanadium thiolate complex $[V(SBu^t)_4]$ was prepared in high yield by treatment of $[VCl_3(THF)_3]$ with $NaSBu^t$ and $Bu^tSSBu^t$ in MeCN(*16*). Treatment of $[VCl_3(THF)_3]$ with $NaSBu^t$ and 2,2′-bipyridine (bipy) led to the ionic species $[V(SBu^t)_2(bipy)_2][V(SBu^t)_4]$ (*16*), which contains the anionic homoleptic derivative $[V(SBu^t)_4]^-$. The structure of the neutral species $[V(SBu^t)_4]$ can again be described as a flattened tetrahedron distorted to $D_{2d}$ symmetry. There are two groups of S—V—S angles, four of average value 107.04(6)° and two of average value 114.45(12)°; the latter (larger) angles are those bisected by the $C_2(S_4)$ axis, which is imposed on the molecule. The four-coordinate V(III) anion $[V(SBu^t)_4]^-$ also has a distorted tetrahedral geometry. However, the S—V—S angles showed that the distortion of the $VS_4$ core from $T_d$ is not analogous to that found in $[V(SBu^t)_4]$. The distortion of the anion was thought due to crystal packing requirements and forces. The V—S bonds (2.280(7)–2.309(7) Å) of the anion are slightly longer than those (2.218(2) Å) in the neutral species, as expected for the lower oxidation state. The neutral homoleptic thiolate complex of the third-row metal tantalum $[Ta(TEMT)_5]$ has been reported briefly from the reaction of $TaCl_5$ with the anion $TEMT^-$ This has the expected trigonal bipyramidal geometry with an average Ta—S distance of 2.37 Å (*12*).

A mononuclear vanadium(III) thiolate species with the relatively small labile ligand THF, $[V(TIPT)_3(THF)_2]$, was prepared by treatment of $[VCl_3(THF)_3]$ with Li(TIPT] in heptane (*17*). An X-ray crystal structure revealed a distorted trigonal bipyramidal geometry about vanadium with the TIPT groups occupying the equatorial positions and the THF molecules filling the axial sites. The TIPT groups dispose their phenyl rings in such a way that two lie on one side and one on the other side of the equatorial plane. This arrangement is a recurring motif in the structures of five-coordinate structures of bulky aromatic thiolates and is evident in structures throughout this review. The distortion from an idealized trigonal bipyramidal structure is evident from an inspection of the S—V—S angles (116.11(3)°, 116.33(3)°, 127.30(3)°). The largest S—M—S angle is between the TIPT ligands, which are on the same side of the equatorial plane, and reflects the steric repulsion between them.

Imido-thiolato-complexes of vanadium of the type $[V(Bu^tN)(SR)_3]$ have been made by the reaction of $[V(Bu^tN)Cl_3]$ with Li[SR] (R = $Bu^t$, $SiPh_3$) (*18*). Comproportionation reactions of the trithiolate with the trihalide precursor were then used to derive the related complexes

$[V(Bu^tN)(SR)_nCl_{3-n}]$ ($n$ = 1,2). Controlled hydrolysis of the trithiolate complex with SR = $SSiPh_3$ gave $[\{V(Bu^tN)(SSiPh_3)_2\}_2O]$, and both this and the trithiolate complex were fully characterized by spectroscopic studies and X-ray structure determinations. It was confirmed that both complexes have distorted tetrahedral arrangements of the ligands around the metal.

## B. Chromium, Molybdenum, and Tungsten

A family of homoleptic four-coordinated pseudo tetrahedral complexes $[Mo(SR)_4]$ has been established employing a range of sterically hindered aromatic and aliphatic thiolate ligands. In contrast, less bulky thiols such as $PrS^-$, $EtS^-$, and $PhS^-$ led only to somewhat poorly defined polymeric products (*19*). The mononuclear homoleptic thiolate complex $[Mo(SBu^t)_4]$ was prepared (*20*) by treating anhydrous $MoCl_4$ with $Bu^tSLi$ in 1,2-dimethoxyethane in about 45% yield. The sulfur atoms around the Mo(IV) have approximately $D_{2d}$ symmetry with two distinct S—Mo—S angles (average 116.9° and 95.6°) and a slightly short Mo—S distance (2.235(3) Å), which is attributed to the low coordination number. The distortion from ideal $T_d$ symmetry to $D_{2d}$ takes the form of an elongation of the tetrahedron, in contrast to $[V(SBu^t)_4]$, which has a flattened tetrahedron. In addition, the disposition of the $SBu^t$ groups is such as to yield an overall symmetry of $D_2$ rather than the $S_4$ reported for $[V(SBu^t)_4]$ (*16*) (shown schematically in Fig. 4).

It was also suggested that the distortion from a regular tetrahedron also accounts for the observed diamagnetism of the $d^4$ complex and reflects the relative magnitudes of the spin-pairing (e.g., Cr > Mo) and ligand field energies (e.g., Mo > Cr) (*20*). The He(1) photoelectron spectrum of $[Mo(SBu^t)_4]$ has been investigated and has been interpreted

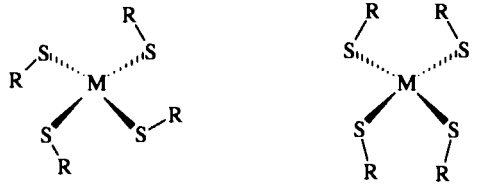


FIG. 4.

by means of MO calculations on the hypothetical molecule $[Mo(SH)_4]$ (*21*). The analogous complexes $[W(SBu^t)_4]$ were prepared by the reaction between $[WCl_4(Et_2S)_2]$ and $Bu^tSH$ at 0°C in toluene in the presence of 4 eq of triethylamine (*22*). An X-ray crystal structure revealed that $[W(SBu^t)_4]$ is isomorphous and isostructural with $[Mo(SBu^t)_4]$. The complex $[Mo(SBu^t)_4]$ exhibited remarkable reactivity toward a range of neutral donor molecules (*20*), but none were simple substitution or addition reactions. Two such reactions are summarized in Eqs. (5) and (6).

$$[Mo(SBu^t)_4] + 4Bu^tNC \longrightarrow [Mo(SBu^t)_2(CNBu^t)_4] + Bu^tS\text{-}SBu^t \quad (5)$$

$$2[Mo(SBu^t)_4] + 2PMe_2Ph \longrightarrow [Mo_2(\mu\text{-}S)_2(CNBu^t)_4(PMe_2Ph)_2] + 2Bu^tSH + 2Me_2C{=}CH_2 \quad (6)$$

The first reaction (Eq. (5)) involves thiolate ligand oxidation with concomitant metal reduction and elimination of disulfide. The second (Eq. (6)) generates a coordinately saturated metal species with bridging sulfur atoms by dealkylation of the $SBu^t$ groups. The analogous complexes with aromatic thiolate ligands were synthesized independently by two groups by quite different routes. The first involved straightforward metathesis of the chloride ligands in $[MoCl_4(THF)_2]$ with the sodium salts of TIPT or TMT (*23*). The other route required the initial synthesis of $[MoCl(TIPT)_4]$ from $MoCl_5$ and $Me_3SiTIPT$, and subsequent reduction (*14*). Although the structure of $[Mo(TIPT)_4]$ was found to be similar to that of $[Mo(SBu^t)_4]$ (*14*), the complex has the capability of forming monoadducts with small molecules, whereas $[Mo(SBu^t)_4]$ does not. Thus the complexes $[Mo(TIPT)_4L]$ (where L = acetylenes, CO or MeCN) could be prepared readily by reaction with the appropriate small molecule, but disappointingly there was no reaction with dinitrogen (*22*). The synthesis of the MeCN adduct also was reported via a one-step reaction from $[MoCl_3(MeCN)_3]$ and the TIPT anion in acetonitrile (*24*). $[Mo(TIPT)_4]$ was also shown to undergo an oxidative addition reaction with diphenyldiazomethane to give the Mo(VI) species $[Mo(=N{-}N{=}CPh_2)(TIPT)_4]$ (*22*). The closely related hydrazido(2-)-complex $[Mo(=N{-}NMePh)(TIPT)_4]$ has been obtained from $MoCl_4$ (NNMePh) and NaTIPT in acetonitrile (*25*).

A systematic investigation of the reactions of $[MBr_2(CO)_4]$ (M = Mo, W) with sterically hindered thiolate ligands led to the series of five-coordinate 14-electron anions $[M(CO)_2(SR)_3]^-$ (SR = TIPT, DIPT, TMT, PFTP) (*26*). This contrasts with the analogous reaction with thiphenol, which gives unstable polymeric species. An X-ray crystal

structure of $[Mo(TIPT)_3(CO)_2]^-$ confirmed that it has a trigonal bipyramidal structure with equatorial thiolate and apical carbonyl groups. Interligand steric repulsion is minimized by the disposition of the thiolates, two of which orientate up, and one down, with respect to the trigonal plane (Fig. 5). One of the carbonyl ligands of $[Mo(TIPT)_3(CO)_2]^-$ could be readily replaced by a range of donor ligands to give species of the type $[Mo(TIPT)_3(CO)L]^-$ (where L = $PMe_2Ph$, $CNBu^t$ and $NCBu^t$) (*27*). The reaction with diazonium salts [PhNN] $[BF_4]$ in acetonitrile resulted in the formation of the neutral species $[Mo(NNPh)(MeCN)(TIPT)_3]$ with a linearly coordinated diazenido(-1) ligand (*28*). Despite the steric congestion $[Mo(TIPT)_3(CO)_2]^-$ is capable of adding a third CO, but the resulting complex slowly decomposes back to the five-coordinate parent complex under an atmosphere of $N_2$ (*27*).

The reaction of $[MoBr_2(CO)_4]$ with the DPT anion (DPT = 2,6-diphenylthiophenolate) differs from that with other 2,6-substituted aromatic thiolates. The stoichiometry $[Mo(DTP)_2(CO)]$ of the product initially suggested three coordination; however, spectroscopic studies and an X-ray crystal structure revealed that one of the 2,6-phenyl groups is $\eta^6$-bonded to the molybdenum (Fig. 6). The $\eta^6$-arene ligand is labile and can be reversibly replaced by three CO ligands. Replacement of this ligand also occurs with 2,2′-bipyridyl (bipy), 1,10-phenanthroline

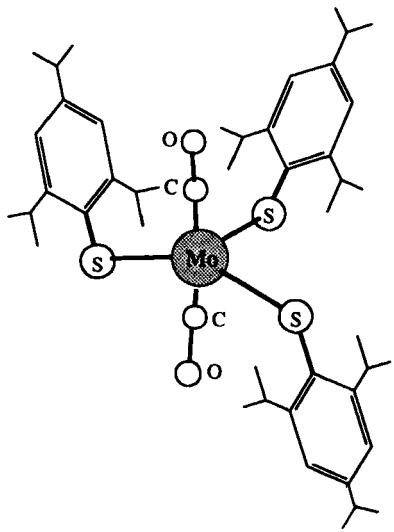


FIG. 5.

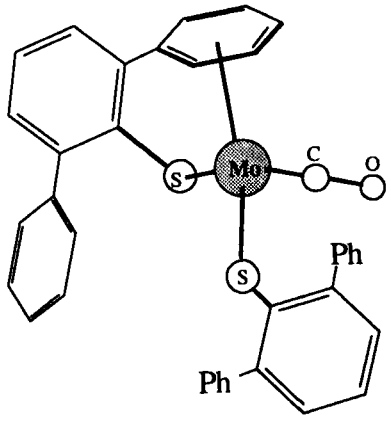


FIG. 6.

(phen), and 1,2-bis(diphenylphosphino)ethane (dppe) to give dicarbonyl complexes of the form $[Mo(DPT)_2(CO)_2L]$ (L = bipy or phen) or the monocarbonyl complex $[Mo(DPT)_2(CO)(dppe)]$, in which the DPT ligands are monodentate (*29*).

The formally Mo(II) trigonal bipyramidal nitrosyl complex $[Mo(TIPT)_3(NH_3)(NO)]$ exhibits the same "one up, two down" configuration of the TIPT ligands with apical ammonia and (linear) nitrosyl ligands (*30*). It was prepared from reaction of the yellow polymeric material "$\{Mo(NH_2O)(NO)\}_n$" (of unknown composition) with excess of the TIPT anion in methanol. The ligated ammonia arose from reduction of the hydroxyl amido-ligand present in the polymeric material. The analogous reaction with the thiolphenolate anion gave the tetrakis thiolate species $[Mo(SPh)_4(NO)]^-$ without the incorporation of ammonia into the coordination sphere (*31*).

The carbyne complexes $[Mo(\equiv CBu^t)(SAr)_3]$ (SAr = TMT, TIPT) have been synthesized by adding 3 eq of Li[SAr] to $[Mo(\equiv CBu^t)Cl_3(dme)]$ (dme = dimethoxyethane). The analogous W derivatives were made by a slightly modified route (*32*). The initial aim was to probe the acetylene metathesis catalytic properties of the complexes $[M(\equiv CBu^t)(SAr)_3]$ (M = Mo, W; SAr = TMT, TIPT). However, none of the complexes were active for metathesis, which was in contrast to the high activity of the analogous alkoxide compounds for metathesis. This was attributed to the stronger electron donation power of thiolate, which reduces the electrophilic nature of the metal center (*32*).

The anionic complexes $[MO(SR)]_4^-$ (M = Mo, W; SR = TEMPT, TIPT) were readily prepared by the reaction of $MoOCl_4$ or $WOCl_4$ with

5 eq of lithium thiolate in $CH_3CN$. The complexes can also be prepared by the reaction of the thiolates with $[MCl_4(CH_3CN)_2]$ in wet $CH_3CN$ (*33*). The X-ray crystal structures of the $[MO(TIPT)_4]^-$ anions (M = Mo, W) showed a square pyramidal arrangement of the ligands about the metal center, analogous to that observed for $[MoO(SPh)_4]^-$ (*34*). Electrochemical studies of these compounds show that they are the central members of a three-membered electron-transfer series (*33*) (Eq. (7)).

$$[M^{VI}O(SR)_4] \overset{E_{ox}}{\rightleftharpoons} [M^{V}O(SR)_4]^- \overset{E_{red}}{\rightleftharpoons} [M^{IV}O(SR)_4]^{2-} \quad (7)$$

The electrochemical reversibility of the M(VI)/M(V) couple for the complexes with sterically hindered ligands contrasts with the reported behavior of the $[MoO(SPh)_4]^-$ complex, which exhibited electrochemical irreversibility for the Mo(V)/Mo(VI) step but a reversible Mo(IV)/Mo(V) couple. The sterically hindered aromatic substituent groups stabilize the molybdenum(VI) complex and decrease $E_{ox}$ relative to the thiophenol derivative. The molybdenum(VI) species can also be isolated by chemical oxidation. $[MoO(PFTP)_4]^{2-}$ was prepared by chemical redution of $[MoO(PFTP)_4]^-$. The presence of the electron-withdrawing substituents on the aromatic thiolate increases $E_{red}$ relative to the thiophenolate derivative. Evidently the properties of these last complexes are influenced primarily by the electron-withdrawing characteristics of the fluorine substituents rather than by steric factors (*33*).

The homoleptic sterically hindered thiolate complex $[Mo_2(TMT)_6]$ containing Mo—Mo triple bonds was first prepared by a multistep reaction (*35*). The X-ray crystal structure showed a staggered configuration for the thiolate ligands with an Mo—Mo distance of 2.228(1) Å (*35*). They were synthesized subsequently by a simple one-step synthesis involving the reaction of $MoCl_4$ with the TIPT anion in 1,2-dimethoxyethane and structurally characterized. A study of their chemistry showed them to be rather unreactive compared with their alkoxide analogues (*36*).

An interesting series of molybdenum and tungsten hydride complexes with sterically hindered thiolate ligands has recently been established due to the interest in their possible relevance to hydrodesulfurization catalysis and to the active site of the enzyme nitrogenase. The complexes $[MH(SAr)_3(PMe_2Ph)_2]$ (M = Mo, W; SAr = TIPT, TMT) were prepared as summarized in Eqs. (8) and (9).

$$[MBr_2(NNH_2)(PMe_2Ph)_3] + 3TIPTH + 2NEt_3 \longrightarrow [MH(TIPT)_3(PMePh)_2] + N_2 + H_2 + PMe_2Ph + 2[NHEt_3]Br \quad (8)$$

$$[WH_6(PMe_2Ph)_3] + 3TIPTH \longrightarrow [WH(TIPT)_3(PMe_2Ph)_2] + 4H_2 + PMe_2Ph \quad (9)$$

The X-ray crystal structures of the complexes $[MH(TIPT)_3(PMe_2Ph)_2]$ (M = Mo, W) have been determined, showing the overall geometry in both cases to be based on a distorted trigonal bipyramidal arrangement of thiolates with the phosphines essentially *trans* to each other. The hydride ligand could not be located by X-ray diffraction in either complex, but its presence was confirmed by IR and NMR spectroscopic studies. Analogous reaction with PhSH gave the nonhydride species $[MoBr(SPh)_3(PMe_2Ph)_2]$ (*37*).

The reaction of $[MoH_4(PR'Ph_2)_4]$ or $[Mo(N_2)_2(PR'Ph_2)_4]$ containing the somewhat bulkier phosphines $PR'Ph_2$ (R' = Me,Et) with 3 eq of TIPTH or TMTH led to the five-coordinate 12-electron species $[MoH(SAr)_3(PR'Ph_2)]$ (SAr = TIPT, TMT). The complexes readily form six-coordinate adducts with ligands such as pyridine and they also catalyze $H_2/D_2$ exchange. The complexes can undergo facile carbon–sulfur bond cleavage to give the sulfur bridged dimers of the type $[\{Mo(SAr)(OMe)(PMePh_2)\}_2(\mu\text{-}S)_2]$, and the derivative with SAr = TIPT was characterized by an X-ray crystal structure (*38*) (Fig. 7). This is a very rare instance of the cleavage of the C—S bond of an aromatic thiolate ligand.

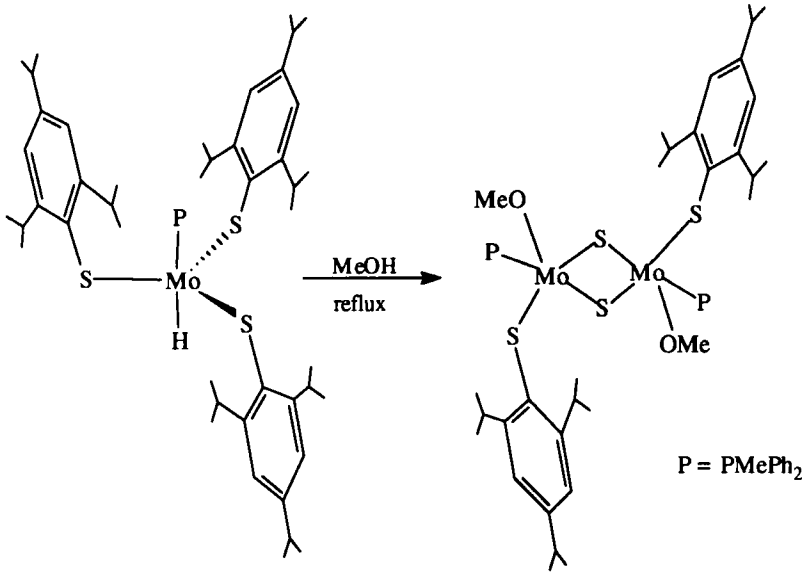


FIG. 7.

## C. Manganese, Technetium, and Rhenium

The homoleptic Mn(III) thiolate complex $[Mn(TIPT)_4]^-$ has been prepared by the reaction of $[MnCl_5]^{2-}$ with excess TIPT anions (*39*). It is believed to have a square planar structure similar to that of $[Co(TIPT)_4]^-$ since they are isomorphous. No further details about its structure have been reported.

The thiol TBTH is considerably more sterically demanding than TIPTH, and treatment of $[Mn\{N(SiMe_3)_2\}]$ with 2 eq of HTBT gives $[\{Mn(TBT)_2\}_2]$. The X-ray crystal structure reveals that it is a well-separated dimer with two bridging thiolates as shown in Fig. 8. Since the molecule has a crystallographic center of inversion, the $[Mn_2S_2]$ core must be planar or nearly planar and each Mn metal is approximately trigonal planar. It is the only three-coordinate open-shell transition metal thiolate complex to be structurally characterized (*40*). Preliminary magnetic data indicated the presence of two high-spin, antiferromagnetically coupled metal centers. This is consistent with the low coordination number and consequently low overall ligand field strength of the coordinating ligands (*40*).

A series of synthetically useful Tc(III) compounds, $[Tc(SAr)_3(MeCN)_2]$ (SAr = TEMT, TIPT), were derived from the reaction of $[NH_4]_2[TcCl_6]$

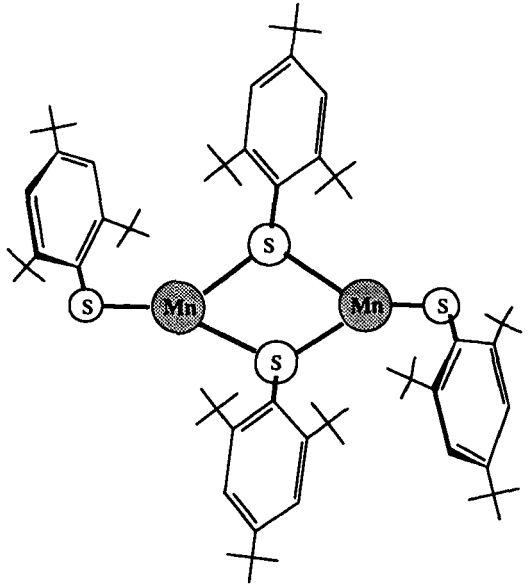


Fig. 8.

with the SAr anion and zinc dust in acetonitrile (*28, 41*). The X-ray crystal structure showed that $[Tc(TEMT)_3(MeCN)_2]$ has a trigonal bipyramidal geometry with equatorial TEMT and axial MeCN ligands. The acetonitrile ligands are readily displaced by small ligands, L (L = CO, $Pr^iCN$, Py), at room temperature to produce the complexes $[Tc(SAr)_3L_2]$ (*28*), isoelectronic and isostructural with the Mo and W complexes discussed above. At elevated temperatures an excess of isocyanide ligands reacted further to produce the well-known Tc(I) complex $[Tc(CNR)_6]^+$ (*28*). One of the carbonyl ligands in $[Tc(SAr)_3(CO)_2]$ is relatively labile and this property was exploited to prepare the monocarbonyl complexes $[Tc(SAr)_3(CO)(MeCN)]$ and $[Tc(SAr)_3(CO)(Py)]$. Both $[Tc(SAr)_3(MeCN)_2]$ and $[Tc(SAr)_3(Py)_2]$ could be oxidized to Tc(V) oxo-species by oxygen atom transfer reactions. The addition of pyridine-*N*-oxide to a refluxing methanolic solution of $[Tc(SAr)_3(MeCN)_2]$ in the presence of excess HAr gave $[Ph_4As][TcO(SAr)_4]$ (*42*). Without the added thiol, the oxidation gave the neutral species $[TcO(SAr)_3(Py)]$. The mass spectrum of $[TcO(SAr)_3(Py)]$ showed that some dimer formation occurred in the FAB matrix, which implied that the loss of the pyridine ligand facilitates dimer formation. $[Tc(SAr)_3(Py)_2]$ is readily oxidized not only by pyridine-*N*-oxide but also by triethylamine-*N*-oxide and DMSO to $[TcO(SAr)_3(Py)]$. $[TcO(SAr)(Py)]$ was shown to be capable of catalyzing the oxidation of $PPh_3$ to $OPPh_3$ by DMSO (*42*).

Reaction of $[n\text{-}Bu_4N][Tc(NO)Cl_4]$ with HTEMT gave $[Tc(NO)(Cl)(TEMT)_3]$ (*43*), which has an IR band at 1798 $cm^{-1}$ characteristic of a linear nitrosyl group, establishing the metal as having a formal oxidation state of +3. The X-ray crystal structure confirmed a trigonal bipyramidal geometry as found for most five-coordinate sterically hindered Tc(III) species.

The reactions between $[TcOCl_4]^-$ and sterically hindered thiolate anions SAr(SAr = TMT, TIPT, DPT) in methanol gave complexes of the type $[TcO(SAr)_4]^-$ (*44*). An X-ray crystallographic analysis revealed that $[Bu_4^nN][TcO(TMT)_4]$ has a square pyramidal geometry with an oxo-group occupying the apical site and the four thiolates, the equatorial sites. The treatment of $[TcO(SAr)_4]^-$ with isocyanide led to loss of a thiolate ligand and reduction of the metal center to Tc(III) via abstraction of the oxo-ligand to form the five-coordinate species $[Tc(SAr)_3L_2]$ (*28, 41*).

In an attempt to prepare $[TcN(TEMT)_4]^-$, the reaction of $[TcNCl_4]^-$ with HTEMT in the presence of the supposedly noncoordinating base 1,1,3,3-tetramethylguanidine (TMG) gave an unexpected complex, *trans*-$[TcN(SC_6HMe_4)_2(NHC(NMe_2)_2)_2]$, with coordinated TMG groups (*45*). The X-ray crystal structure showed a square pyramidal structure

with an apical Tc≡N bond. The alternative nitrido-complex precursor $[TcN(OH)(Py)_4]^+$ reacted with an excess of HTEMT to produce only a bis(thiolato) complex, *trans*-$[TcN(TEMT)_2(Py)_2]$, which contrasts with the formation of the tris(thiolate) complex $[TcO(TEMT)_3(Py)]$ under similar conditions from an pyridine oxo-complex (*45*). It appears that nitrido-Tc complexes tend to have less affinity for ligated SAr ligands than comparable mono-oxo Tc complexes.

The chemistry of some Re nitrosyl complexes provided a striking example of the differences between sterically hindered and unencumbered aromatic thiolates (*46*) (Eqs. (10) and (11)).

$$[ReCl_2(OCH_3)(NO)(PPh_3)_2] + PhS^- \longrightarrow [Re_2(SPh)_7(NO)_2]^- \quad (10)$$

$$[ReCl_2(OCH_3)(NO)(PPh_3)_2] + TIPT^- \longrightarrow [Re(TIPT)_4(NO)] \quad (11)$$

Treatment of the nitrosyl $[ReCl_2(OMe)(NO)(PPh_3)_2]$ with thiophenol yielded a triply thiolate-bridged dimer, whereas the bulkier TIPTH gave the monomer $[Re(TIPT)_4(NO)]$. The latter reaction involves oxidation of Re(II) to Re(III) in the presence of excess TIPT anions. This is unusual in the view of the well-known tendency of the thiolate anion to reduce the metal, but probably reflects the facile oxidation of the possible intermediate $[Re(NO)(TIPT)_4]^-$. The crystal structure of $[Re(TIPT)_4(NO)]$ revealed the favored tbp geometry with equatorial thiolate ligands.

The bis-acetonitrile complexes $[Re(NCCH_3)_2(SAr)_3]$ (SAr = DIPT, TIPT, TMT) were synthesized from $[ReCl_6]^{2-}$ and excess thiolate anion in acetonitrile (*47*). The Re complexes are structurally analogous to $[Tc(MeCN)_2(SAr)_3]$ and the substitution chemistry of both species with CO is directly analogous. The related complex $[Re(SAr)_3(MeCN)(PPh_3)]$ was prepared from $[ReCl_3(MeCN)(PPh_3)_2]$ and an excess of the thiolate anion (*47*). Under the same conditions, 2-trimethylsilythiophenol gave an unexpected complex, $[Re(SC_6H_4\text{-}2\text{-}SiMe_3)\{NC(SC_6H_4\text{-}2\text{-}SiMe_3)CH_3\}_2(PPh_3)_2$ (*48*). The most unusual feature of the complex is the presence of thiolimidate groups $[N{=}C(SC_6H_4\text{-}2\text{-}SiMe_3)CH_3]^-$, formed by nucleophilic attack on the coordinated nitrile by mercaptide.

The five-coordinate Re(V) oxo-complexes $[ReO(SAr)_4]^-$ (SAr = TIPT, DIPT, TMT, TEMT, DPT) have been obtained by reaction of $[ReOCl_3(PPh_3)_2]$ with an excess of thiolate anions. The X-ray crystal structures of $[ReO(DIPT)_4]^-$ and $[ReO(TMT)_4]^-$ have been determined (*49*). Both complexes have pyramidal geometries with apical oxo atoms and are structurally analogous to the anions $[MoO(SPh)_4]^-$ and $[TcO(TEMPT)_4]^-$. The anion $[ReO(TIPT)_4]^-$ was accompanied by the un-

usual cation $[Ph_3PTIPT]^+$, the $PPh_3$ arising from the Re precursor. The complex $[ReO(SPh)_4]^-$ is readily reduced by $Ph_3P$ in acetonitrile to $[Re(SPh)_3(PPh_3)(MeCN)]$, but by contrast, $[ReO(SAr)_4]^-$ failed to react with phosphines. This may be attributed to shielding by the sterically hindered thiolate ligands, which protect the oxo-ligand from attack.

The reactions of sterically hindered thiolate anions with rhenium precursors containing a multiply bonded nitrogen have also been studied (*47*). The reaction of $[ReNCl_2(PR'_3)_n]$($PR'_3$ = $PPh_3$, $n$ = 2, or $PMe_2Ph$, $n$ = 3) with the bulky thiol HTIPT under varying conditions gave the nitrido-complexes $[ReN(TIPT)_4]^{n-}$ ($n$ = 1,2) and of these $[ReN(TIPT)_4]^-$ was actually isolated. The monoanion is a paramagnetic rhenium(VI) complex derived from the aerial oxidation of the rhenium(V) anion $[ReN(TIPT)_4]^{2-}$ (*47*). The related arylimido Re(V) complexes $[PPh_4][Re(NR'')(TIPT)_4]$ (R''=Ph, $C_6H_4OMe$-4, or $C_6H_4Me$-4) can be isolated by the reaction of $[Re(NR'')Cl_3(PPh_3)_2]$ with HTIPT and triethylamine (*47*). The $^1H$ NMR spectroscopic data are consistent with square pyramidal geometries with apical multiply bonded nitrogen ligands, which are structurally analogous to $[ReO(SAr)_4]^-$. However, the reactions of $[Re(NPh)Cl_3(PPh_3)_2]$ or $[ReNCl_2(PPh_3)_2]$ with sterically undemanding thiophenolate anion gave products containing no nitrogen. This indicates that the sterically hindered aromatic thiolates stabilize the complexes with metal nitrogen multiple bonds.

The reactions of aromatic sterically hindered thiolates with rhenium hydride precursors are highly dependent on the nature of the substituents and the conditions employed. Thus $[ReH_7(PPh_3)_2]$ reacted with DMTH in toluene at room temperature to give $[Re(DMT)_3(PPh_3)]$ together with a second minority product, $[Re(DMT)_3(PPh_2H)(PPh_3)]$ (*50*). The former complex was shown by X-ray crystallography to have a pseudo-trigonal bipyramidal structure with an agostic interaction with a hydrogen of a DMT methyl in an axial site (Fig. 9). The latter derivative also has a trigonal bipyramidal structure, with the two phosphine ligands in apical sites. The formation of the secondary phosphine ligand presumably involved the elimination of benzene via reaction with a hydrido-species (*50*).

In the analogous reactions of $[ReH_7(PPh_3)_2]$ with TIPTH, the dinitrogen complex $[Re(TIPT)_3(N_2)(PPh_3)]$ is generated in high yield in toluene at room temperature under dinitrogen. An X-ray crystal structure (Fig. 10) showed a trigonal bipyramidal structure with equatorial thiolates. Due to the bulk of the triphenylphosphine ligand, the aromatic thiolate groups are all directed to the opposite side of the equatorial plane and form a cavity within which the $N_2$ ligand is located (*51*). Significantly the $N_2$ complex could also be prepared by the reaction of [Re

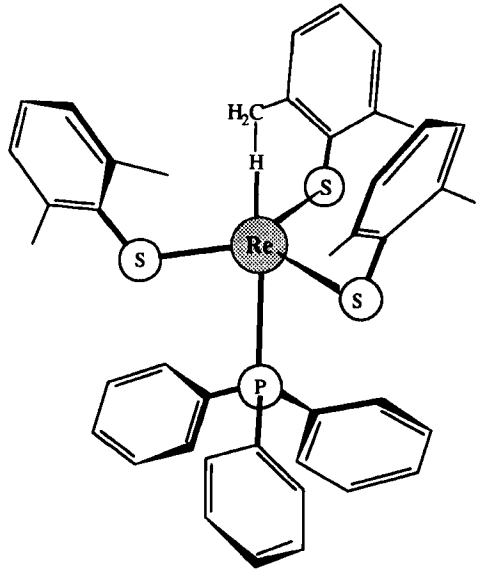


FIG. 9.

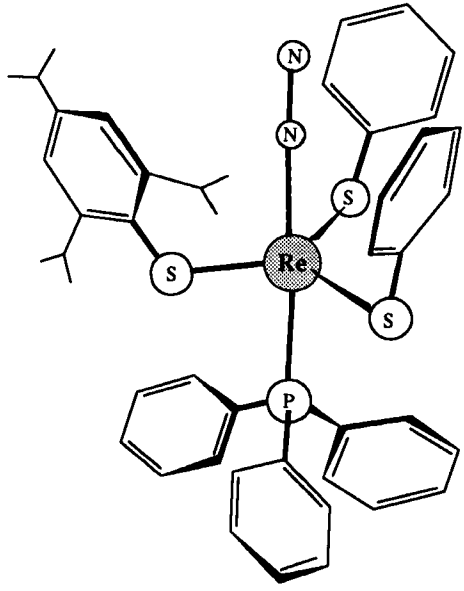


FIG. 10.

$OCl_3(PPh_3)_2$] with sodium borohydride and thiolate in toluene, without the necessity of isolating the intermediate hydrido-complex. The dinitrogen is readily replaced by a variety of neutral donors (CO, MeCN, etc.), and $Bu^tNC$ displaces both $N_2$ and the $PPh_3$ to give [Re(TIPT)$_3$ ($Bu^tNC$)$_2$]. In this last complex the steric interplay between the bulky isocyanide and TIPT groups produces a unique conformation of the TIPT aromatic groups, as shown schematically in Fig. 11, and the molecule is chiral.

The mechanism of the reaction is at present unclear, and the only hydride intermediate that can be identified by $^{31}P$ and $^1H$ NMR is $[ReH_4(PPh_3)_4]^+$. This complex was isolated as a salt in conjunction with the known $[ReO(TIPT)_4]^-$ anion by reaction of $[ReH_5(PPh_3)_3]$ with TIPT in toluene, or from $[ReH_7(PPh_3)_2]$ and $PPh_3$ together with $[HPPh_3][BF_4]$, and has been characterized by X-ray crystallography (*50*).

## D. Iron, Ruthenium, and Osmium

The rubredoxin metalloprotein features a [Fe(S-cys)$_4$] unit, and there have been intensive efforts to synthesize stable $[Fe(SR)_4]^{n-}$ ($n$ = 1,2) complexes to serve as synthetic analogues. The homoleptic tetrathiolate Fe(III) complexes $[Fe(TMET)_4]^-$ and $[Fe(TIPT)_4]^-$ were first prepared from the reactions of $FeCl_3$ with the appropriate sterically hindered thiolate anions in dry methanol (*52–54*). In contrast to the sterically hindered thiolate ligands, thiophenolate gives the Fe(II) anion $[Fe(SPh)_4]^{2-}$. The failure to isolate $[Fe^{III}(SPh)_4]^-$ in this reaction was ascribed to the tendency of any $[Fe(SPh)_4]^-$ complex formed to oligomerize and/or undergo autoredox reactions to Fe(II) and RSSR, which was thought to involve bridging thiolate ligand intermediates. However,

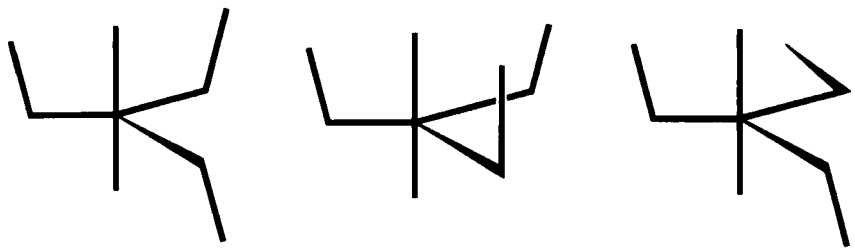

(a) (b) (c)

Fig. 11.

the complex $[NEt_4][Fe(SPh)_4]$ was shown to be accessible by the reaction of $[NEt_4][Fe(2,6\text{-dimethylphenolate})_4]$ with excess benzenethiol in DMF at 0°C, followed by the addition of diethyl ether. An X-ray diffraction study confirmed that it possesses an overall distorted tetrahedral geometry. For each Fe—SPh group, the Fe—S bond lies in the plane determined by the phenyl ring (*52*). In contrast the planes of the phenyl rings in $[Fe(SAr)_4]^-$ (SAr = TEMT, TIPT) are perpendicular to the Fe—S bond. Evidently the sulfur $p$-$\pi$ lone pair orbitals are conjugated with the phenyl rings in $[Fe(SPh)_4]^-$ but are orthogonal to them in $[Fe(SAr)_4]^-$. The 2,6-substituents prevent the sulfur $p$ orbitals conjugating with the thiolate phenyl rings. The effect that this can have is demonstrated by a comparison of the $Fe^{3+}/Fe^{2+}$ redox potentials of $[Fe(TEMT)_4]^-$ (−0.85v vs SCE) and $[Fe(SPh)_4]^{2-}$ (−0.52v). The 3+ oxidation state was clearly more stable in the TEMT complexes, again confirming the propensity of the bulky thiolates to stabilize metals in higher oxidation states (*54*). Although the orientation of the aryl groups is important in determining the redox characteristics, the establishment of a hydrophobic environment about the metal is also a significant contributing factor.

The Fe(III) complex $[Fe(TEMT)_4]^-$ has $S_4$ crystallographic symmetry that makes it particularly suitable for single crystal polarized absorption, MCD, and EPR spectroscopic studies. A bonding model that permitted a correlation to be made between the structural variations and the observed spectra was derived. The spectra were also compared in detail with that of an oxidized rubredoxin (*55*). Analogous spectroscopic studies have also been made on single crystals of the Fe(II) species $[Fe(2\text{-}PhC_6H_4S)_4]^{2-}$. The nature of the ground state was shown to be strongly dependent on the orientation of the sulfur substituent (*56*). The X-ray crystal structures of the series of complexes $[M(2\text{-}PhC_6H_4S)_4]^{2-}$ have been determined and all have $S_4$ crystallographic symmetry and tetragonally compressed $MS_4$ cores (*57*).

Bulky aromatic thiolates have also been used to modify the redox potentials of cubane-type $Fe_4S_4$ clusters (*58, 59*). High potential iron-sulfur proteins (HIPIP) have $[Fe_4S_4(S\text{–}Cys)_4]^{2-/1-}$ cores but the 2−/1− redox process is not generally observed for conventional $[Fe_4S_4(SR)_4]^{2-}$ clusters containing nonsterically hindered thiolate ligands. Nevertheless, these can be accessed by use of an unusual electrolyte/solvent system (*60*). However, the complexes $[Fe_4S_4(SAr)_4]^{2-}$ (SAr = TMT, TIPT) are known and serve as models for the HIPIP metalloproteins. $[Fe_4S_4(TMT)_4]^{2-}$ was prepared from the reaction of ferric chloride in methanol with 3 eq of THT anion, followed by 1 eq of a methanolic solution of sodium hydrosulfide and sodium methoxide (*59*). Alterna-

tively $[Fe_4S_4(TIPT)_4]^{2-}$ was synthesized by a ligand exchange method from the precursor $[Fe_4S_4(SBu^t)_4]^{2-}$ (*58*). Both complexes exhibited electrochemically quasi-reversible $2-/1-$ redox couples at $+0.02$v and $-0.03$v vs SCE, respectively, whereas the $3-/2-$ couple was electrochemically irreversible (*59*). The complexes $[Fe_4S_4(SAr)_4]^{2-}$ (SAr = TMT, TIPT) exhibit very strong ligand–metal charge transfer (LMCT) absorption maxima at 412 nm (for TMT) and 413 nm (for TIPT). These are blue shifted from the 457-nm peak observed for $[Fe_4S_4(SPh)_4]^{2-}$, which contrasts to the red shifts observed for the complexes $[Fe_4S_4(SAr)_4]^{2-}$ (SAr = 2-S-tolyl, 4-S-tolyl) containing *ortho* or *para* electron-donating substituents in the thiolate phenyl rings. An X-ray diffraction study of $[Et_4N]_2[Fe_4S_4(TMT)_4]$ rationalized these phenomena (*61*). The molecular structure of $[Fe_4S_4(TMT)_4]^{2-}$ showed that the $[Fe_4S_4]^{2+}$ core has a cubane structure almost identical to that of the analogous $[Fe_4S_4(SPh)_4]^{2-}$. However, the mean Fe—S bond length (2.274 Å) in the TMT derivative is longer than that (2.263 Å) of $[Fe_4S_4(SPh)_4]^{2-}$, and the Fe—S—C(Ph) bond angles (100.4°, 99.4°) are smaller than those found for $[Fe_4S_4(SPh)_4]^{2-}$ (*62*). Such parameters indicate a reduction in the overlap between the $p$-$\pi$ orbitals of the thiolato sulfur and the $d$ orbitals of Fe, which parallels the behavior observed for the $[Fe(SAr)_4]^{n-}$ complexes above.

The electrochemical study showed that the $[Fe_4S_4(SAr)_4]^{-}$ complexes (SAr = TMT, TIPT) are stable after generation by electrochemical oxidation. The oxidized species $[Fe_4S_4(SAr)_4]^{-}$ was also shown to be accessible by the direct chemical oxidation of $[Fe_4S_4(SAr)_4]^{2-}$ with $[(C_5H_5)_2Fe][BF_4]$ (*59*). The crystal structure of $[Fe_4S_4(SAr)_4]^{-}$ revealed that the cubane-like $[Fe_4S_4]$ core is tetragonally compressed with four short Fe—S bonds and eight long Fe—S bonds (*59*). Furthermore the average Fe—S (2.26 Å) and Fe—S(R) (2.21 Å) bond distances are similar to those determined from the X-ray crystal structure of the $[Fe_4S_4]^{3+}$ center of the oxidized HIPIP. The shift to longer wavelength of the lowest energy band in the electronic spectrum of $[Fe_4S_4(SAr)_4]^{2-}$ upon oxidation to $[Fe_4S_4(SAr)_4]^{-}$ parallels the behavior observed for HIPIP metalloproteins. There have also been some detailed studies of the Mössbauer and EPR spectra of the oxidized clusters, and again strong similarity to the oxidized HIPIP proteins was observed (*63*).

Treatment of $[NEt_4]_2[Fe_2S_2Cl_4]$ with TMT anion in acetonitrile led to formation of $[NEt_4][Fe_2S_2(TMT)_4]$ (*64*). The X-ray crystal structure revealed that the complex contains a planar $Fe_2S_2^{2+}$ core. Two of the four Fe—S(C) torsion angles rotate from the stable staggered to the eclipsed conformation due to steric congestion. The eclipsed Fe—S(C) unit has a wide Fe—S—C angle [112.35(76)°], whereas the staggered

Fe—S(C) unit displays a narrower Fe—S—C angle [104.95(64)°], suggesting a difference in $\pi$-bonding between the two types of thiolate ligand.

The compound [{Fe(TBT)$_2$}$_2$], an analogue of [{Mn(TBT)$_2$}$_2$], was synthesized by treatment of [Fe{N(SiMe$_3$)$_2$}$_2$ with 2 eq of HSAr (*40*). The iron complex is isomorphous and isostructural to [{Mn(TBT)$_2$}$_2$]. The Fe—Fe distance is 3.202 Å, which is significantly shorter than the Mn—Mn distance of 3.554 Å (*40*).

The thiolate chemistry of the congeners of iron in Group VIII has, as expected, been shown to be quite distinct from that of iron. Thus the tetrathiolate complexes [M(SAr)$_4$(MeCN)] (M = Ru, Os; SAr = TEMT, TIPT) were prepared from the reaction of [Et$_4$N][RuCl$_4$(CH$_3$CN)] with 4 eq of LiSAr and 0.5 eq of ArSSAr in refluxing methanol–acetonitrile solution (*65*). In view of the high formal oxidation state of the metals and the reducing capacity of the thiolate ligands, the complexes [M(SAr)$_4$(MeCN)] are surprisingly thermally and air stable in solution as well as in the solid state. The X-ray crystal structure of [Ru(TEMT)$_4$(MeCN)] shows a TBP geometry with the MeCN axis (*65*). The ligated MeCN was found to be readily replaceable by CO to give [M(SAr)$_4$(CO)] (M = Os, Ru; SAr = TEMPT, TIPT), in which the binding of CO to the metals is unusual in view of the high oxidation state of the metals [M(IV)]. It was proposed that Sp$\pi$—Md$\pi$ bonding enhances the $\pi$ basicity of the metals so as to stabilize the $\pi$-acidic carbonyl ligands. The analogous selenium complexes [Ru(Se-2,3,5,6-Me$_4$C$_6$H)$_4$(CH$_3$CN)] and [Ru(Se-2,3,5,6-MeC$_4$H)$_4$(CO)] have also been prepared (*66*). The $\nu$(CO) values in the IR spectra for these complexes indicated that the sulfur ligands were better electron donors than their selenium counterparts.

An X-ray crystallographic analysis of [Ru(TEMT)$_4$(CO)] revealed that the metal has the same trigonal bipyramidal geometry as the parent MeCN complex (*66*). Interestingly, the orientation of the equatorial thiolate ligands shows subtle differences between the carbonyl and the MeCN complexes. In the case of the [Ru(TEMT)$_4$(NCCH$_3$)], two arenes point toward the acetonitrile ligand and one away (two up, one down configuration). The [Ru(TEMT)$_4$(CO)] complex has all three equatorial thiolate aryl groups pointing toward the carbonyl ligand (three up configuration). However, the $^1$H NMR spectra indicate that both types are present in solution and are not interconverting rapidly on the NMR time scale.

A series of intriguing complexes [Ru(SR)$_4$(NO)]$^-$ [SR = TEMT, DMT, TIPT) were prepared from the reaction of K$_2$[Ru(NO)Cl$_5$] with a range of aromatic thiolate anions (*67*). The compounds demonstrated several

unusual features: low NO IR stretching frequencies (1720–1740 $cm^{-1}$), despite the electron configuration of the $[Ru(NO)]^{3+}$ core; the ease with which the NO could be displaced; and the subtle dependence of reactivity on the thiolate substituents.

The complex $[Ru(NO)(TIPT)_4]^-$ is readily converted into $[Ru(TIPT)_4L]$ (L = MeOH, DMSO, $CH_3CN$) simply by heating it under reflux in the appropriate solvent. The mild conditions required for this NO displacement reaction appear to be unprecedented for a $[Ru(NO)]^{3+}$ center. It was proposed that the redox stability of the $[Ru^{IV}(SR)_4L]$ product provides the driving force for the displacement reaction. Subsequent removal of bonded MeOH from $[Ru(TIPT)_4MeOH]$ by a pyrolysis reaction gave $[Ru(TIPT)_4]$. The X-ray crystal structure revealed the complex to be pentacoordinate rather than four coordinate, the additional coordination being provided by an agostic interaction between the Ru and a methine C—H of an ortho isopropyl group, as shown in Fig. 12 (*67*). This is in direct contrast with the complex $[Mo(TIPT)_4]$, which has a straightforward four-coordinate geometry. Less sterically hindered thiolates such as DMT displayed a different reactivity pattern, and $[Ru(TEMT)_4(NO)]$ underwent a cyclometalation reaction upon heating in methanol to give a novel binuclear complex in which two [Ru(NO)] units are retained (*67*). The C—H bonds of 2-methyl groups of two of the thiolate ligands are activated to give a cyclometallated product. The X-ray crystal structure shows that the complex has three bridging TEMT ligands, as shown in Fig. 13. One of them is a normal bridging TEMT ligand, but the others have additional Ru—C $\sigma$ bonds,

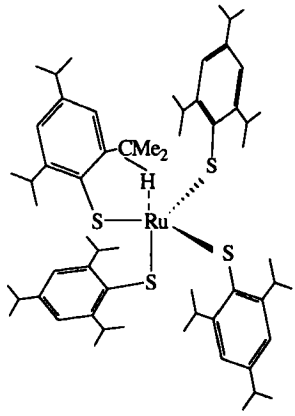


FIG. 12.

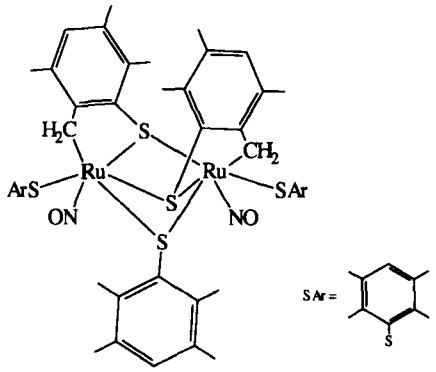


FIG. 13.

via 2-methyl substituents, to form five-membered ring systems. Each Ru atom has an overall distorted octahedral geometry.

The use of Ru(II) and Ru(III) halido-tertiary phosphine complexes as precursors has provided a route to a diversity of Ru thiolate derivatives. The product of the reaction of $[RuCl_n(PR_3)_3]$ ($PR_3$ = $PPh_3$, $n$ = 2; $PMe_2Ph$, $n$ = 3) is controlled by the nature of both the thiolate and the phosphine ligands. With $C_6F_5SH$ (PFTPH), $[RuCl_2(PPh_3)_3]$ forms $[Ru(PFTP)_2(PPh_3)_2]$, in which there are strong interactions between 2-hydrogens on phosphine phenyl groups with the metal center (*68*). Under similar conditions two of the smaller $PMe_2Ph$ ligands are retained upon reaction with $[RuCl_3(PMe_2Ph)_3]$ to give $[Ru(PFTP)_3(PMe_2Ph)_2]$. In this complex one of the 2-fluoro-groups on the thiolate interacts with the metal to give distorted octahedral coordination of the metal (*68*) (Fig. 14). For osmium, depending on the precursor used, both

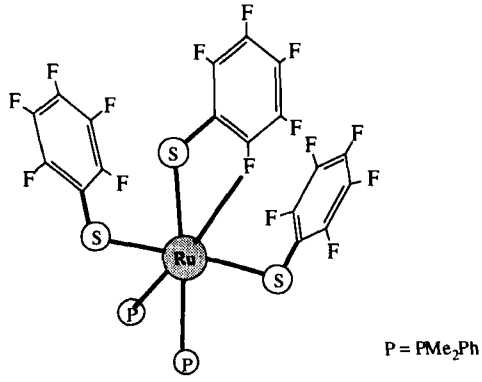


FIG. 14.

$[OsCl(PFTP)_3(PMe_2Ph)]$ and $[Os(PFTP)_3(PMe_2Ph)_2]$ are known. The former has a trigonal bipyramidal structure with the Cl and $PMe_2Ph$ groups in the axial sites (*69*).

The reaction of 2,6-diphenylthiophenol (DPTH) with $[RuCl_2(PPh_3)_3]$ in methanol in the presence of base results in a complex of stoichiometry $[Ru(DPT)_2(PPh_3)]$. An X-ray crystal structure of this complex showed $\eta^6$-bonding of one of the thiolate phenyl substituents, to give an overall geometry very similar to that of the Mo complex described above (*70*). A directly analogous Os complex was prepared in similar fashion from DPTH and $[OsCl_2(PPh_3)_3]$ (*70*).

### E. Cobalt, Rhodium, and Iridium

The nature of the products of the reactions of $CoCl_2$ with bulky aromatic thiols in acetonitrile has been shown to be dependent on both the ratio of thiolate anion to $CoCl_2$ used and the bulk of the substituents (*71*). With TEMT and an S:Co ratio of 3:1, the four-coordinate complex $[Co(TEMT)_3(NCCH_3)]^-$ was generated, whereas under similar conditions, thiophenolate anions gave $[Co_4(SPh)_{10}]^{2-}$. The lower S:Co ratio of 2:1 gave a complex of formula $[Co(TEMT)_2]$, whereas the higher S:Co ratio of 8:1 gave $[Co(TEMT)_4]^{2-}$. $[Co(TEMT)_3(NCCH_3)]^-$ was fully characterized by an X-ray crystal structure determination. The bond angles of the $CoS_3N$ unit show large deviations from ideal tetrahedral angles of 109.5°, which was attributed to the mixed coordination sphere and steric interactions among the ligands.

The reaction of $CoCl_2$ with 5 eq of Li[TIPT] in EtOH gave a brown solution, and oxidation with oxygen gave a deep red solution. Subsequent addition of $[PPh_4]Br$ permitted the isolation of deep red $[Co(III)(TIPT)_4]^-$, which provides an unusual example of a square planar Co(III) complex (*72*) (Fig. 15). The change in structure upon moving from tetrahedral $[Co(TMT)_4]^{2-}$ to the Co(III) complex was attributed to the larger ligand field splitting associated with a metal in the trivalent state (*72*). The average Co—S bond distance of 2.207(3) Å in $[Co(TIPT)_4]^-$ is about 0.1 Å shorter than that found in $[Co(TMT)_4]^{2-}$. Interestingly the Co(III) complex with TEMT was markedly less stable than that with TIPT and provides a further example of increasing steric bulk stabilizing higher oxidation states. This may well in part reflect a reduction in the formation of thiolate bridged intermediates necessary for electron transfer and reduction, as discussed in Section IIID for iron.

The efforts to synthesize cobalt species containing two thiolate ligands was stimulated by the fact that catalytic zinc in liver alcohol dehydrogenase (LADH) is coordinated by two cysteines, and cobalt-

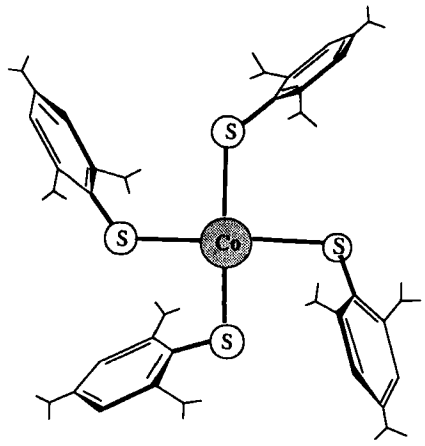


FIG. 15.

substituted LADH is quite similar to the native zinc enzyme in terms of structure and activity (*73*). Complexes of the type $[Co(TIPT)_2L_2]$ (L = $NCCH_3$, pyridine, imidazole) were synthesized from $[Co(TIPT)_2]$ and the appropriate nitrogen base (*73*). An X-ray crystallographic study of $[Co(TIPT)_2py_2]$ showed that it possesses a distorted tetrahedral structure, which closely resembles the $[(Cys–S)_2Zn(imid)(his)]$ (imid = imidazole, his = histidine) coordination unit of the structurally characterized imidazole-inhibited enzyme. Under similar conditions, bidentate ligands such as bipyridine or phenanthroline gave five-coordinated complexes of the form $[Co(TIPT)_2L(NCCH_3)]$ (L = bipy, phen) (*73*). The X-ray crystal structure of $[Co(DIPT)_2(bpy)(NCCH_3)]$ shows a distorted trigonal bipyramidal geometry. The bipy ligand spans an axial–equatorial edge while the $CH_3CN$ occupies the remaining axial position. Tuning the size of the bidentate ligand by using the more sterically hindered 2,9-dimethyl-1,10-phenanthroline discourages five coordination and the X-ray structure of $[Co(DIPT)_2(2,9\text{-}Me_2phen)]$ confirmed that a four-coordinate complex was indeed generated (*73*).

However, as observed elsewhere, the slightly less steric hindered thiolate TEMT ligands display rather different chemistry in analogous reactions. The resultant complex is a dimer, $[\{Co(TEMT)_2(bipy)\}_2]$, with two five-coordinate cobalts linked by two asymmetric thiolate bridges, as shown in Fig. 16 (*73*).

The binuclear derivative $[\{Co(SAr)_2\}_2]$ (SAr = TBT), an analogue of $[\{M(TBT)_2\}]$ (M = Mn, Fe), was prepared via the same route as $[\{Fe(TBT)_2\}_2]$ (*40*). The metal–metal distance in the Co complex (2.222 Å)

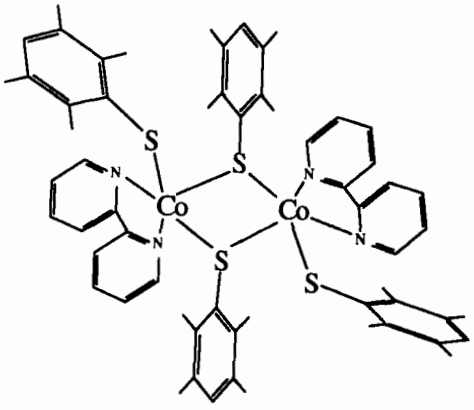


FIG. 16.

is the shortest of the series of complexes of the type $[\{M(TBT)_2\}_2]$ (M = Mn, Fe, Co).

The reactions of $RhCl_3$ with a range of sterically hindered thiolates in MeCN revealed some interesting variants on the theme of the interactions of 2,6-substituents of aromatic thiolates with a metal center. The dinuclear species $[Rh_2\{\mu\text{-}SC_6H_3(2\text{-}C_6H_4)\text{-}6\text{-}Ph\}_2(DPT)_2(NCCH_3)_2]$ was prepared from the reaction of $RhCl_3$ with DPT in MeCN in the presence of $Et_3N$ as base (*29*). The overall structure is shown in Fig. 17 and reveals that each bridging thiolate ligand is also $\sigma$-bonded to

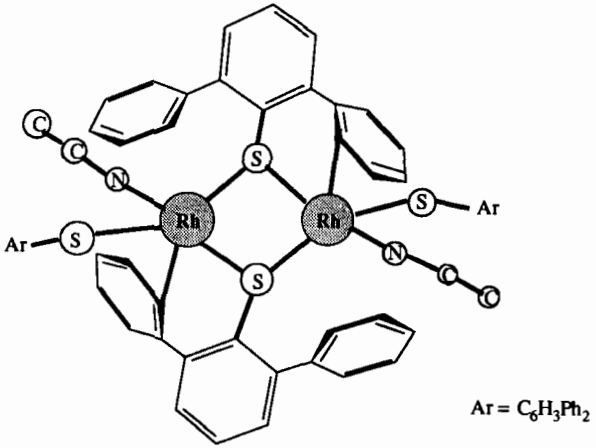


FIG. 17.

a rhodium atom (Rh—C distance, 2.016(8) Å) via one of the phenyl carbons of the thiolate substituents. Each Rh atom is five coordinate with square pyramidal geometry, the basal plane comprising two bridging thiolate sulfur atoms, the sulfur of the terminal thiolate ligand, and the nitrogen of the acetonitrile ligand. The $\sigma$-bonded carbon occupies the axial site. A distinctive feature of this complex is that the Rh atoms lie within the basal plane to produce a planar $[Rh(\mu\text{-}S)_2(S)(N)]$ moiety. This contrasts with the commonly observed displacement of the metal from the basal plane toward the apical ligand in square pyramidal complexes such as $[PPh_4][MoO(SCH_2CH_2CH_2S)_2]$ (0.76 Å) (*74*), $[PPh_4][ReO(TMT)_4]$ (0.71 Å) (*49*), and $[PPh_4][ReS(SCH_2CH_2S)_2]$ (0.40 Å) (*75*). These observations support the notion that the magnitude of metal ion displacement from the basal ligand plane depends on the nature of the M—L apical bond. Thus small multiply bonded ligands such as oxo- and sulfido- generate significant displacements, whereas a $\sigma$-bonded apical ligand, such as in this rhodium dimer system, generates little or no deviation.

The reaction of $RhCl_3$ with an excess of the anion of TIPT in MeCN also generated a dinuclear complex in high yield, in which the bridging aromatic thiolate also binds via an arene substituent, but in this case the two rhodium atoms are not equivalent (*76*). A representation of the overall crystal and molecular structure is shown in Fig. 18. A simplified view of the coordination sphere of one rhodium atom is shown in Fig. 19. The structure comprises two distinct metal atoms, with

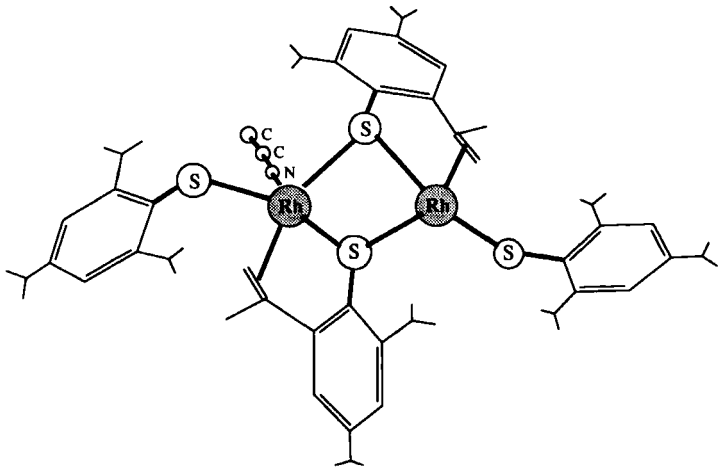


FIG. 18.

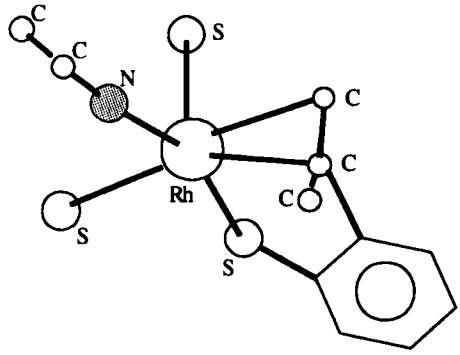


FIG. 19.

pseudo-octahedral ligation about one Rh atom and pseudo-trigonal bipyramidal geometry about the other. The Rh atoms each have a formal oxidation state of 2 and are bridged by two thiolato-sulfur atoms. One isopropyl group on each bridging thiolato-ligand has been dehydrogenated to give a $CMe{=}CH_2$ unsaturated group $\eta^2$-bonded to rhodium, as shown in Fig. 17. The Rh—C distances lie within the range found for other rhodium–alkene complexes, and the Rh—Rh distance of 2.750(1) Å is indicative of a single Rh—Rh bond.

The thiolate chemistry of the lower oxidation states of Rh and Ir is dominated by the formation of oligomers with bridging thiolates, even when these bear bulky or electron withdrawing substituents. A typical precursor for access to Rh(I) chemistry is $[Rh_2Cl_2(COD)_2]$ (COD = 1,8-cyclooctadiene), and successive treatment with PFTPH and CO gave $[Rh_2(PFTP)_2(CP)_4]$ with bridging PFTP ligands (*77*). An extensive investigation has been made of Ir(I) complexes of the type $[Ir_2(\mu\text{-}SBu^t)_2(CO)_2(PR_3)_2]$ and their catalytic activity studied in depth (*78*). Replacement of one of the bridging thiolates by pyrazole leads to a further series of dimeric comples that are active as hydroformylation catalysts and can be protonated to give derivatives with both bridging and terminal hydride ligands (*79*). Mononuclear hydrido-complexes are comparatively rare for these elements, perhaps due to the facile migration of hydride to the thiolate sulfur and the elimination of the free thiol. However, reaction of $[IrCl_3(PMePh_2)_3]$ with 2-triphenylsilylthiophenol (TPSTPH) in the presence of triethylamine in methanol gave $[IrH(TPSTP)_2(PMePh_2)_3]$. An X-ray crystal structure revealed pseudo-octahedral coordination about the Ir with *mer*-$PMePh_2$ and *cis*-thiolate ligands. The hydride ligand was not observed, but is presumably located in the vacant site *trans*- to one of the thiolate sulfurs (Fig. 20) (*80*).

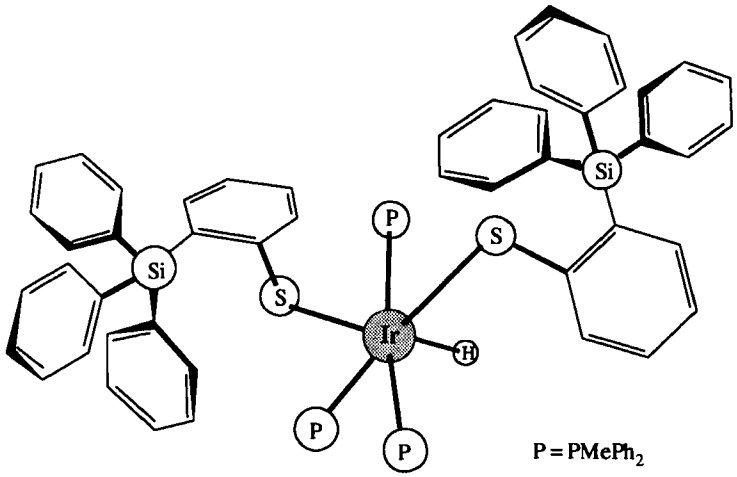


FIG. 20.

## F. NICKEL, PALLADIUM, AND PLATINUM

Nickel has been one of the more recent additions to the list of transition metals crucial to the activity of metalloproteins, and spectroscopic studies on the nickel-containing active site(s) of several hydrogenases have indicated the presence of S donor atoms in the first coordination sphere of the nickel center (*81*). This has stimulated a good deal of work on the thiolate chemistry of nickel, but there is to date comparatively little reported work on sterically hindered thiolate complexes of Ni. The five-coordinate Ni complex, [Ni(terpy)(TIPT)$_2$] (terpy = 2,2′:6′,2″-tripyridine, a tridentate ligand) has been synthesized from the reaction of [Ni(terpy)Cl$_2$] with [Me$_4$N][TIPT] in MeCN (*82*). Under the same reaction conditions, the PFTP anion gave the solvated octahedral complex [Ni(terpy)(PFTP)$_2$(NCCH$_3$)], whereas thiophenolate anion produced the bridged species [{Ni(terpy)(SPh)$_2$}$_2$] (*82*). The overall geometry of the complex [Ni(terpy)(TIPT)$_2$] is distorted trigonal bipyramidal with the two bulky thiolate ligands coordinated in the equatorial plane. One hydrogen of a Pr$^i$-group from each TIPT ligand has a short approach (ca. 3.0–3.5 Å) to the nickel metal center, which prevents the metal from acquiring another ligand. The EPR spectra of the solution of the complex reduced with dithionite under a CO atmosphere confirmed that reduction had occurred, and the product was proposed to be [Ni(terpy)(TIPT)$_2$(CO)]$^-$. When [Ni(terpy)(TIPT)$_2$] was treated with NaBH$_4$ in DMF the resultant product was presumed to be [Ni(terpy)

$(TIPT)_2(H)]^-$, based on the study of its EPR spectra. This behavior is consistent with observations of the binding of CO and $H^-$ to nickel in the nickel-containing enzyme.

The coordination chemistry of palladium and platinum with large aromatic thiolates has been restricted to some studies with PFTPH, although there is an extensive reported chemistry of oligomeric complexes with smaller thiols. Halide complexes of Pd and Pt were shown to react with Tl(PFTP) to give the presumably monomeric, square planar anionic M(II) complexes $[M(PFTP)_4]^{2-}$ (*83*).

## G. Copper, Silver, and Gold

The chemistry of copper with sterically hindered thiolates is dominated by linear two coordination and the simplest example is provided by $[Cu(TEMT)_2]^-$, prepared from the reaction of $[Cu(NCMe)_4][BF_4]$ with excess TEMT anion (*71*). The linear coordination of the Cu(I) ion was confirmed by X-ray crystallography. Although the complex $[PPh_4][Cu(SPh)_2]$ has been reported, it was not structurally characterized (*71*). The chemistry of $[PPh_4][Cu(SPh)_2]$ differs significantly from that of $[Cu(TEMT)_2]^-$ in that $[Cu(SPh)_2]^-$ readily undergoes oligomerization reactions in solution to give cluster compounds such as $[Cu_4(SPh)_{10}]^{2-}$ and $[Cu_5(SPh)_7]^{2-}$ (*84–86*).

However, a series of $[Cu(SAr)]_n$ ($n$ = 4, 8, 12) clusters have been obtained from the reaction of various sterically hindered thiolate anions with appropriate metal precursors. The degree of aggregation of these is, as expected, strongly and directly dependent upon the bulk of the thiolate ligand, and the larger the ligand, the smaller the value of $n$. The smallest clusters so far characterized have $n$ = 4, and $[Cu_4(BSTP)_4]$ (BSTPH = $HSC_6H_3$-2,6-$(SiMe_3)_2$) was synthesized from the reaction of BSTPH with $[Cu(CH_3CN)_4]PF_6$ in methanol (*87*). The structure was determined by X-ray diffraction methods and is shown schematically in Fig. 21. The core of the molecule comprises an nonplanar eight-membered $Cu_4S_4$ ring of alternating Cu and S atoms and the four Cu atoms form a distorted rhombus, with each Cu having linear coordination. The $Cu_4S_4$ unit is distinctly folded about the $S_2$—$S_4$ axis to produce a dihedral angle of 134.0° between the best planes through $S_2$—$Cu_3$—$S_3$—$Cu_4$—$S_4$ and $S_2$—$Cu_2$—$S_1$—$Cu_1$—$S_4$.

The reaction of CuCl with HTIPT produced an octamer $[Cu_8(TIPT)_8]$ (*88*), which is one of two isomeric forms, and the structure of isomer 1 is shown in Fig. 22, which omits the aromatic groups for clarity. The core of isomer 1 of the $[Cu_8(TIPT)_8]$ cluster consists of a twisted 16-membered cyclic aggregate of alternating copper and doubly bridging

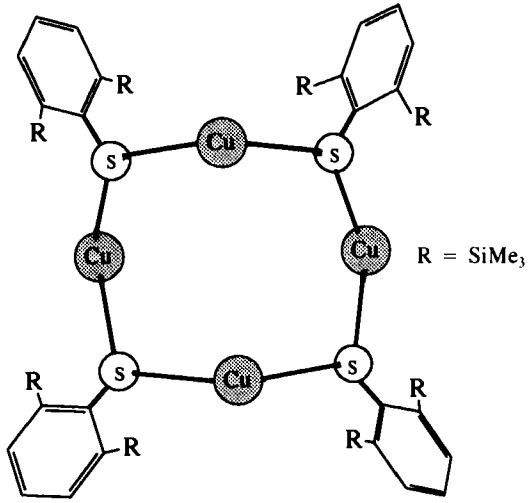


FIG. 21.

sulfur atoms, and as usual each copper atom exhibits linear two coordination. However, reaction of TIPTH with the different precursor $CuCO_3 \cdot Cu(OH)_2$ under milder conditions gave $[Cu_4(TIPT)_4]$ (*89*). The structure of this tetramer is directly analogous to that of $[Cu_4(BSTP)_4]$. Furthermore, protracted reaction times promote the formation of a second isomer of the octameric cluster $[Cu_8(TIPT)_8]$ (isomer 2) (*89*). A schematic version of the molecular structure appears in Fig. 23. It has a $Cu_8S_8$ core, consisting of a folded 16-membered Cu—S ring with the symmetry $C_2$. The eight S atoms are arranged at the corners of two cubes, with Cu atoms occupying eight of the edges.

As the overall size of the thiolate is decreased, the degree of aggregation increases, and the reaction of $[Cu(MeCN)_4][PF_6]$ with STPH

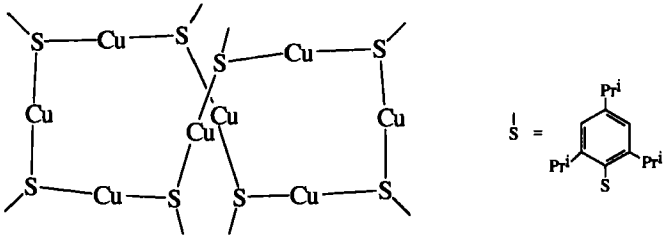


FIG. 22.

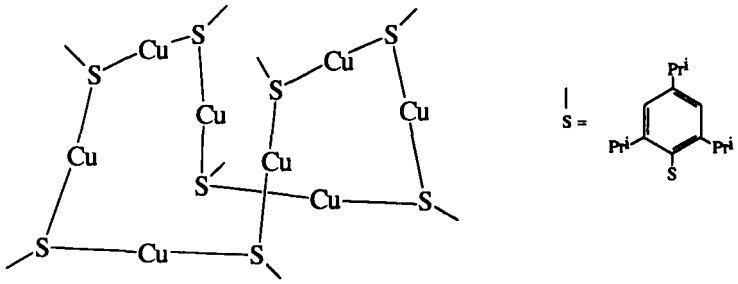


FIG. 23.

(STP = 2-(trimethylsily)benzenethiol) affords red–orange crystals of $[Cu_{12}(STP)_{12}]$, a dodecameric thiolate cluster (*87*). The structure of $[Cu_{12}(STP)_{12}]$ can be described as a molecular paddle wheel, with the $Cu_{12}S_{12}$ core illustrated in Fig. 24. Both linear and trigonal planar geometries are found for Cu in the structure. It is unusual to find both types of coordination in the same molecule, but there is precedent for these geometries in copper–thiolate clusters (*88, 91*).

As described in Section II, an extensive series of sterically hindered alkyl thiols containing the bulky silyl, $—SiR_1R_2R_3$, group have been synthesized. The coordination of these to Ag(I) to give clusters of the type $[Ag(SR)]_n$ provided a unique opportunity to fine-tune the substituents to control the degree of aggregation. Thus $[Ag_3(SC(SiPhMe_2)_3)_3]$ consists of a cyclic trinuclear structure (*8*), whereas $[Ag_4(SC(SiMe_3)_3)_4]$ has a cyclic tetranuclear structure (*8*). The less-hindered ligand $—SCH(SiMe_3)_2$ produced a novel bis-cyclic structure $[\{Ag_4(SCH(SiMe_3)_2)_4\}_2]$ (*8*), which consists of two $Ag_4S_4$ rings linked together by

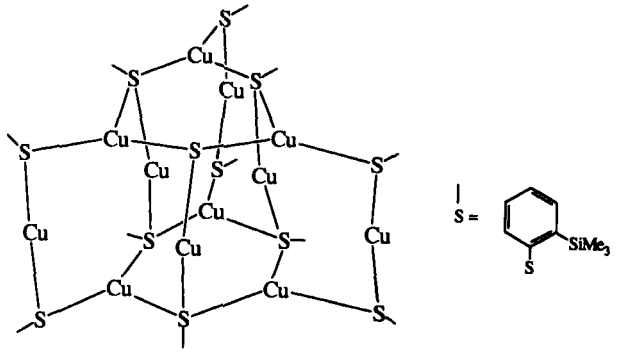


FIG. 24.

secondary Ag—S interactions to produce a bis-cyclic structure. Further reduction in ligand bulk gave only infinite polymers.

The steric demands of the silylated aromatic thiolate STPH are similar to those of the aliphatic thiolate ligand —$SCH(SiMe_3)_2$, and treatment of $AgNO_3$ with $STP^-$ in acetonitrile gave the bis-cyclic structure $[\{Ag_4(STP)_4\}_2]$ (*11*), shown in Fig. 25. The $Ag_4(STP)_4$ unit is directly analogous to that found in the equivalent copper complex and consists of a folded eight-membered ring of alternating silver and sulfur atoms. The steric hindrance exerted by the STP ligands is insufficient to prevent close approach of the two $[Ag_4S_4]$ units to form secondary Ag—S interactions with a distance of 3.053(7) Å between the two rings. The resulting bis-cyclic structure is shown schematically in Fig. 24. The geometry about two of the Ag atoms is distinctly T-shaped rather than trigonal planar, but the rest adopt a linear coordination. Although both $[\{Ag_4(STP)_4\}_2]$ and $[\{Ag_4(SCH(SiMe_3)_2)_4\}_2]$ have bis-cyclic structures, there are some significant differences between the two. Thus all eight Ag centers of the aliphatic thiolate species display T-type coordination, whereas the STP complex has only two such centers. The orientation of all four substituents of the aliphatic thiolates are directed to the same side of one face of the first ring away such that they point away from the second ring to give an *aaaa* configuration. By contrast the STP complex has an *aaab* configuration by virtue of the disposition of three thiolate ligands on the first ring to point away from the second ring, but a fourth ligand points in the diametrically opposite sense (*11*).

The analogous chemistry of gold has been less well explored, but the cluster $[Au_6(TIPT)_6]$ has been reported as the product from the reaction

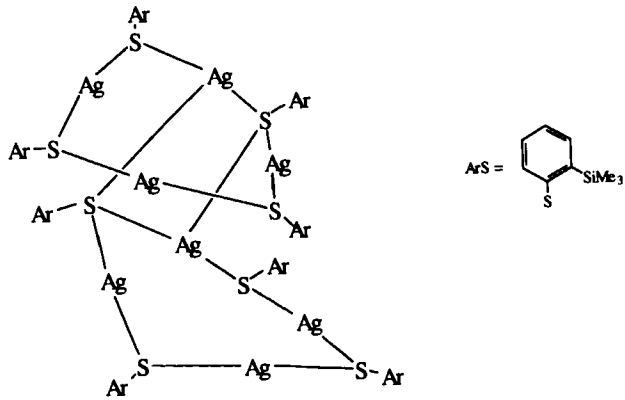


FIG. 25.

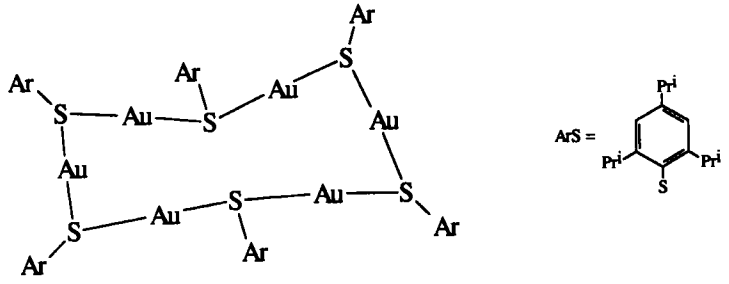


FIG. 26.

of Au(CO)Cl with TIPTH in ether (*92*). The X-ray crystal and molecular structure showed a centrosymmetrical 12-membered Au—S ring in the chair conformation with linearly coordinated Au atoms at the midedges and S atoms at the corners, and is shown in abbreviated form in Fig. 26. However, the monomeric species $[Au(TIPT)_2]^-$ can be prepared by using liquid ammonia as a solvent for the reaction of AuI with TIPTH (*92*). The gold atom in $[Au(TIPT)_2]^-$ is as expected linearly coordinated and the complex is essentially isostructural with $[Cu(TEMT)_2]^-$, discussed above.

## H. ZINC, CADMIUM, AND MERCURY

The principal impetus to the study of zinc thiolates has undoubtedly been the search for structural models for the metal coordination in zinc metalloproteins such as the $Zn(S–Cys)_2(His)_2$ center in the transcription factor IIIA and other "zinc fingers" that feature in protein–DNA interactions (*93, 94*). The 2:1 complexes $[M(SR)_2]$ (M = Zn, Cd; SR = TIPT, TEMT) were used as the principle precursors for the synthesis of such models for the $Zn(S\text{-}Cys)_2(His)_2$. Thus complexes of the types $[Cd(TIPT)_2(1\text{-}CH_3\text{-}imid)_2]$, $[Zn(TIPT)_2(bipy)]$, and $[Zn(TEMT)_2(1\text{-}CH_3\text{-}imid)_2]$ (imid = imidazole, bipy = bipyridine) were synthesized by addition of a nitrogeneous base to the precursor in MeCN. All of them have been characterized by X-ray crystallography and were found to have distorted tetrahedral geometries. It was noticed that the cobalt analogue binds a solvent molecule MeCN to form five-coordinate $[Co(TIPT)_2(bipy)(CH_3CN)]$, whereas $[Zn(TIPT)_2(bipy)]$ does not (*96, 97*).

$[Zn(TBT)_2(Et_2O)]$ was prepared from the reaction of $[Zn(CH_2SiMe_3)_2]$ with 2 eq of HTBT in the presence of ether (*98*). The X-ray crystal structure shows the zinc to have a T-shaped planar three-coordinate geometry, with a S—Zn—S angle of about 160° and the shortest Zn—S

distance (ca. 2.196 Å) thus far observed for Zn—S bonds. The short Zn—S bonds suggest that the Zn—S bonding orbitals probably have approximate sp hybridization. In the absence of $Et_2O$, the reaction gave a white precipitate of $Zn(SAr)_2$ (*98*). This was believed to be monomeric in $C_6D_6$, based on $^1H$ NMR spectroscopy and cryoscopy. Owing to its low coordination and relative electron deficiency, the Zn center can behave readily as an acceptor toward suitable electron donors such as a single $Et_2O$ molecule.

$[Zn(TEMT)_3]^-$ has been synthesized by the reaction of $ZnSO_4$ with 5 eq of Li[TEMT] in $CH_3CN$ (*99*), and the X-ray crystal structure confirmed three coordination of the zinc with a significant distortion from three-fold symmetry. The sum of the three S—Zn—S angles equals 360.0°, indicative of a planar $ZnS_3$ coordination. The coordination of the Zn metal center is best described as a Y-shape, which has one large S—Zn—S angle (134.10(8)°) and a long Zn—S distance (2.243(2) Å) (opposite to the large angle) compared with the other two (2.217(2) Å, 2.230(2) Å). Although three coordination is common for $d^{10}$ transition metal ions such as Hg(II), Cu(I), and Ag(I) (*100*), it is relatively rare for both Zn(II) and Cd(II). The absence of the solvated adduct, $[Zn(TEMT)_3(NCCH)_3]^-$, in the synthetic reaction is in marked contrast to cobalt, for which $[Co(TEMT)_3(CH_3CN)]^-$ has been identified. Although MeCN cannot apparently bind to $[Zn(TEMT)_3]^-$, 1-methylimidazole (1-Me-imid) will join with $[Zn(TEMT)_3]^-$ to form $[Pr_4^nN][Zn(TEMT)_3(1\text{-Me-imid})]$ (*99, 101*). This served as a model compound for the $[Zn(S\text{-cys})_3(his)]$ coordination found in gene 32 and other proteins. The $ZnS_4$ core is also accessible, and $[Zn(TEMT)_4]^{2-}$ has been synthesized by the reaction of $ZnCl_2$ with 8 eq of K[TEMT] in $CH_3CN$ and has been structurally characterized (*99*). The average Zn—S distance increases systematically along the series $[Zn(TEMT)_3]^-$ (2.23(1) Å), $[Zn(TEMT)_3(1\text{-Me-imid})]$ (2.33(2) Å), and $[Zn(TEMT)_4]^{2-}$ (2.36 Å).

An attempt to prepare the Cd analogue of $[Zn(TEMT)_3]^-$ gave the dimeric, thiolate bridged compound $[Pr_4^nN]_2[Cd_2(TEMT)_6]$ (*102*). However, more bulky thiolate ligands such as TIPT and TBT can generate the three-coordinate complexes $[Cd(SAr)_3]^-$ (SAr = TIPT, TBT) (*102, 103*), and the synthesis of the complexes $[Hg(SAr)_3]^-$ (SAr = TIPT, TEMT) has also been achieved from a mercuric halide (*102, 103*). The X-ray crystal structure of $[PPh_4][Cd(TIPT)_3]$ has been determined, and the $[Cd(TIPT)_3]^-$ anion has approximately $C_{3h}$ symmetry and is shown in Fig. 27. The individual S—Cd—S angles are close to 120° and the sum of the three angles is 360°, consistent with trigonal planar coordination of the Cd. However, the coordination about the Cd is a function of packing effects within the crystal, and changing the cation causes

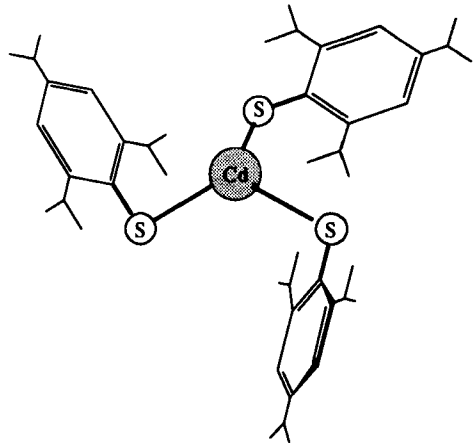


FIG. 27.

significant distortions. Thus the X-ray structure of the complex $[Bu_4^nN][Cd(TIPT)_3]$, reveals a Y-shaped geometry about the Cd.

Similar variations of geometry have been observed for the analogous complexes of Hg. Thus the X-ray crystal structures of $[Pr_4^nN][Hg(TIPT)_3]$ and $[Ph_4P][Hg(TEMT)_3]$ revealed Y-shaped coordination, whereas the anion of $[Ph_4P][Hg(TIPT)_3]$ was believed to have $C_{3h}$ symmetry, based on $^{199}Hg$ CP/MAS–NMR. The $C_{3h}$ symmetry isomers are characterized by all S—M—S angles being equal to ca. 120° and nearly equal M—S bond distances. The Y-shaped isomers are characterized by a wider range of S—M—S angles, with one S—M—S angle greater than 120° (ca. 134°–137°). The M—S bond that is opposite the large angle is found to be longer than the other two. The Y-shaped isomer has been proposed (*103*) to be an intermediate structure along the pathway toward the formation of a linear two-coordinate complex by the dissociation of the third thiolate ligand. The linear complex $[Hg(TIPT)_2]$ has also been obtained by variation of the workup procedure for the reaction to synthesize the $[M(TIPT)_3]^-$ anions (*103*).

Recently the reactions of cyclohexylthiol (CHEXTH) with mercuric halides have been studied, and it was shown that treatment of $HgBr_2$ with a large excess of CHEXTH gave the novel cluster $[Hg_7(CHEXT)_{12}Br_2]$. Suitable crystals for an X-ray diffraction study were grown from pyridine, and the core structure is shown in simplified form in Fig. 28, the thiolate cyclohexyl substituents having been omitted for clarity. A central Br atom is surrounded by an irregular octahedron of Hg atoms, with the unusual feature that the Br is octahedrally coordinated.

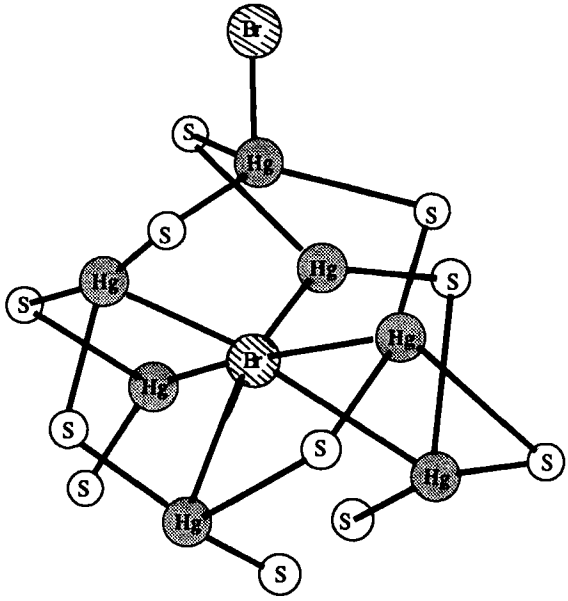


FIG. 28.

Six of the seven Hg atoms have very distorted four-coordinate geometries with one short and two long Hg—S distances and a long Hg—Br distance (*104*).

The complexes $[\{Cd(EC_6H_2Bu_3^t)_2\}_2]$ (E = S, Se) formally contain two-coordinate Cd and have been synthesized from the reaction of the bulky chalcogen ligand with $[Cd\{N(SiMe_3)_2\}_2]$ (*105*). Unlike the related complexes, $[\{M(TBT)_2\}_2]$ (M = Mn, Fe, Co), the X-ray crystal structure of $[\{Cd(TBT)_2\}_2]$ reveals two asymmetrically bridging thiolato-ligands with the $Cd_2S_2$ four-membered rings forming a planar parallelogram. However, the compound was believed to be monomeric in solution based on $^1H$ NMR spectroscopic studies. This is in contrast to $[\{M(TBT)_2\}_2]$ (M = Mn, Fe, Co), which remains dimeric in solution (*40*).

The trinuclear cluster anion $[Cd_3(TIPT)_7]^-$ was prepared by the straightforward reaction of $Cd(NO_3)_2$ with 3.2 eq of TIPTH and $Et_3N$ in MeOH (*106*). The X-ray crystal structure of the anion is shown in Fig. 29. The core of the anion consists of a defective cubane-like $Cd_3S_4$ unit with three doubly bridging thiolate and one triply bridging thiolate ligands. Each cadmium atom exhibits tetrahedral coordination with one terminal thiolate sulfur, two doubly bridging thiolate sulfurs, and a triply bridging thiolate sulfur. This is the first example of a disubsti-

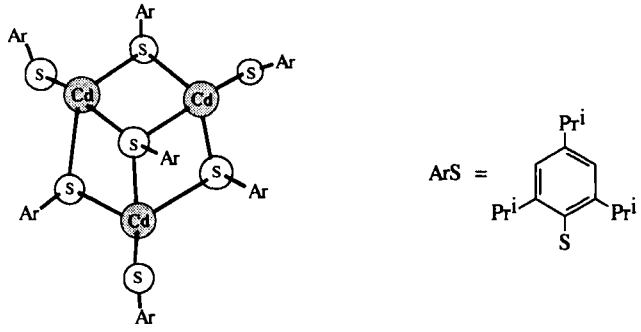


FIG. 29.

tuted aromatic thiolate ligand functioning in a triply bridging mode. It was suggested that this cluster provides a relevant model for the structure of the Cd(II)-cysteinate aggregate in metallothioneins.

## IV. Main Group Complexes

The chemistry of the main group elements with sterically demanding thiols has not in the past received the same level of attention as that of the transition metals, but there has been a recent surge of interest in this area. Thus $[Li(THF)_3(TBT)]$ has been prepared quantitatively from the reaction of free TBTH with Bu$^n$Li in THF (*13*) and provides a rare example of a monomeric Li derivative. The X-ray crystal and molecular structure confirmed tetrahedral coordination about the Li with three THF molecules and a TBT ligand. It is in interesting contrast to the dimeric structures found for $[\{Li(Et_2O)(O\text{-}2,6\text{-}Bu_2^t\text{-}4\text{-}MeC_6H_2)\}_2]$, $[Li_2(THF)_{3.5}\{SC(SiMe_3)_3\}_4]$, and $[Li_2(THF)_4\{SCH(SiMe_3)_2\}_4]$ (*107, 108*).

The coordination chemistry of the group (III) metals Al and Ga with the thiols TBTH, TIPT, and TEMT has been investigated. The reaction of HSAr (SAr = TIPT, TEMT) with $GaCl_3$ in the presence of base gave the tetrahedral derivatives $[Ga(SAr)_4]^-$ (*109*). In contrast, reaction of the trihalides with Li[TBT] under similar conditions gave the three-coordinate neutral complexes $[M(TBT)_3]$ (M = Al, Ga) (*110*). The X-ray crystal structures of $[M(TBT)_3]$ (M = Al, Ga) display an almost planar trigonal $MS_3$ core with the metal atoms located slightly above the plane of the three sulfur atoms. The aromatic rings of the TBT ligands form an irregular propeller-like arrangement around the $S_3$ plane. Furthermore there are three short M—H distances between the metal and one of

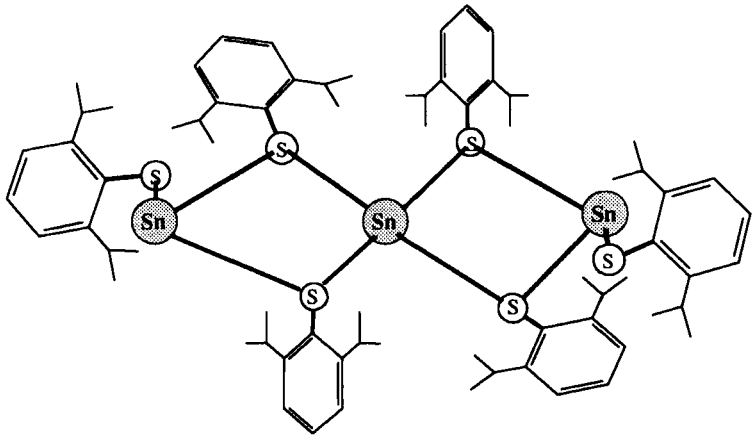


FIG. 30.

the 2-butyl substituents (Al—H = 2.72, 2.841, 2.969 Å; Ga—H = 2.691, 2.91, 2.973 Å).

In an effort to increase hydrocarbon solubility and to impose unusually low coordination numbers on complexes of Group (IV)B metals, the derivatives $[M(SAr)_2]$ (M = Ge, Sn, Pb; SAr = TBT) and $[M_3(SAr)_6]$ (M = Ge, Sn, Pb; SAr = DIPT) have been synthesized by the reactions of the M(II) chlorides with excess of the appropriate thiolate anions (*111*). The X-ray crystal structure of $[Sn(TIPT)_2]$ showed it to be monomeric and essentially V-shaped with an S—Sn—S angle of 85.4(1)°. The tin atom can alternatively be regarded as having trigonal coordination, with a lone pair of electrons occupying one of the coordination sites. The structure of $[Sn_3(DIPT)_6]$ is illustrated in Fig. 30. The terminal Sn atoms have a tetrahedral geometry with a lone pair, whereas the central Sn atoms have a distorted trigonal bipyramidal geometry with an equatorial lone pair. It is interesting that the presence of the $Pr^i$ group in the 4 position is able to generate the monomeric two-coordinate species. It illustrates that relatively subtle steric effects remote from the metal can determine the structure.

## V. Conclusions

The deployment of sterically hindered thiolate ligands has considerably increased the scope of metal sulfur coordination chemistry over the past 10 years. The primary emphasis has been on aromatic thiols

as these show little tendency to undergo C—S bond cleavage reactions. An essential requirement of this chemistry is the systematic variation of the size and nature of the aromatic subtituents. In this context the new high-yield synthetic route via lithiation of thiophenol developed by Block and Zubieta is significant as it offers the possibility of the facile introduction of one or two silylated substituents in the 2 and 6 positions on the aromatic ring. The majority of aromatic thiolates investigated have symmetrical 2,6-substitution, but from some recent results it appears that just one substituent is sufficient to ensure that thiolate bridges do not form, and some new types of complex can be isolated. Aliphatic thiolates with C—SH bonds have been little studied with the exception of $Bu^tSH$ due to the ease of cleavage of the C—S bond. The advent of bulky silyl thiols may well promote further work in this area as, although hydrolytically sensitive, the Si—S bond is reasonably robust under anhydrous conditions.

The most prevalent coordination numbers for transition metals are 4 and 5, although the largest thiols are able to generate three-coordinate metal ions, albeit in thiolate bridged dimers. Higher coordination numbers are generally possible only with small molecules such as $H_2$, $N_2$, and CO as coligands. Although many of the complexes are nominally coordinatively unsaturated, the electron-deficient metals have a high tendency to interact with the 2,6-substituents on the thiolate aryl groups. This can involve agostic M—H interactions or in some cases a fully fledged C—M $\sigma$ bond. With 2,6-diphenylthiophenol, a labile $\eta^6$ arene complex can be formed, and displacement of this group provides access to three coordination sites at the metal. This concept of functional substituents is potentially one of the most promising areas of development in this chemistry. The substituent may interact relatively weakly with the metal (OMe, $C_6H_5$, etc.) and can function as a protecting group for the metal until another substrate molecule is presented. If the substituent is a strong donor ($Ph_2P$, etc.), then stable chelated derivatives are produced. These can offer distinct advantages in terms of catalysis involving hydrides as elimination of the free thiol by hydride migration to sulfur will be reduced by chelation.

The bulky aromatic thiolate ligands are capable of stabilizing higher oxidation states than might at first sight be expected in the presence of the reducing thiolate anion. The mechanism of this stabilization appears to be a combination of steric and electronic effects. The electron density at a thiolate coordinated metal is a sensitive function of the orientation of the aromatic group with respect to the S—C bond vector, as this also determines the degree of $S\pi$—$d\pi$ bonding between sulfur and the metal. It is also possible that the creation of a strongly hydro-

phobic environment for the metal may also modify the redox properties of the complexes. Whatever the balance between these two factors, systematic variation of the substituents offers a means to fine-tune the redox properties of a metal complex and this will doubtless be exploited further in the future.

It is hoped that this chapter will serve to summarize the synthetic methods and structural patterns that underlie this relatively new facet of coordination chemistry and will stimulate further research in this interesting area. The ability of sterically hindered thiols to generate mononuclear species with unusual geometries and oxidation states has arguable relevance to the metal sites found in metalloproteins with cysteine coordination, and this theme will doubtless be pursued further. There appears to be little doubt that whatever the impetus for the chemistry, many new and interestingly reactive complexes will emerge, and that some of these will be capable of interacting with small molecules and will be active for a variety of catalytic and stoichiometric transformations.

## REFERENCES


1. Blower, P. J., and Dilworth, J. R., *Coord. Chem. Rev.* **76,** 121 (1987).
2. Dance, I. G., *Polyhedron* **5,** 1037 (1986).
3. Krebs, B., and Henkel, G., *Angew. Chem., Int. Ed. Engl.* **30,** 769 (1991).
4. McAuliffe, C. A., and Murray, G. G., *Inorg. Chim. Acta Rev.* **6,** 103 (1972).
5. Stiefel, E. I., *Prog. Inorg. Chem.* **22,** 1 (1977).
6. Newman, M. S., and Karnes, H. A., *J. Org. Chem.* **31,** 3980 (1986).
7. Grunwald, F. A., *J. Org. Chem.* **16,** 945 (1951).
8. Tang, K., Aslam, M., Bloch, E., Nicholson, T., and Zubieta, J., *Inorg. Chem.* **26,** 1488–1497 (1987).
9. Bloch, E., Eswarakrishan, V., Gernon, M., Ofori-Okai, G., Saha, C., Tang, K., and Zubieta, J., *J. Am. Chem. Soc.* **111,** 658 (1989).
10. Bloch, E., and Aslam, M., *Tetrahedron* **44,** 281 (1988).
11. Bloch, M., Gernon, M., Kang, H., Ofori-Okai, and Zubieta, J., *Inorg. Chem.* **28,** 1263–1271 (1989).
12. Corwin, D. T., Jr., Corning, J. F., and Millar, M., *191st Am. Chem. Soc. Natl. Meet.,* New York, *1986,* Abstr. 147 (1986).
13. Sigel, G. A., and Power, P. P., *Inorg. Chem.* **26,** 2819–2822 (1987).
14. Roland, E., Walborsky, E. C., Dewan, J. C., and Schrock, R. R., *J. Am. Chem. Soc.* **107,** 5795.16 (1985).
15. Dufee, L. D., Latesky, S. L., Rothwell, I. P., Huffman, J. C., and Folting, K., *Inorg. Chem.* **24,** 4596 (1985).

15a. Bochmann, M., Hawkins, I., and Wilson L., *J. Chem. Soc., Chem. Commun.,* p. 344 (1988).

15b. Coucouvanis, D., Hadjikkyriacou, A., and Kanatzidis, M. G., *J. Chem. Soc., Chem. Commun.,* p. 1224 (1985).

15c. Coucouvanis, D., Lester, R. K., Kanatzidis, M. G., and Kessigoglou, D., *J. Am. Chem. Soc.* **107,** 8279 (1985).
16. Heinrich, D. D., Folting, K., Huffman, J. C., Reynolds, J. G., and Christou, G., *Inorg. Chem.* **30,** 300 (1991).
17. Randall, C. R., and Armstrong, W. H., *J. Chem. Soc., Chem. Commun.*, p. 986 (1988).
18. Preuss, F., Noichl, H., and Kaub, J., *Z. Naturforsch., B: Anorg. Chem., Org. Chem.* **41B,** 1085 (1986).
19. Dilworth, J. R., Blower, P. J., and Bishop, P. T., unpublished results (1983).
20. Otsuka, S., Kamata, M., Hirotsu, K., and Higuchi, T., *J. Am. Chem. Soc.* **103,** 3011 (1981).
21. Takahashi, M., Watanabe, I., Ikeda, S., Kamata, S., and Otsuka, S., *Bull. Chem. Soc. Jpn.* **55,** 3757 (1982).
22. Dewan, J. C., Roland, E., Walborsky, E. C., Wigley, D. E., and Schrock, R. R., *Inorg. Chem.* **26,** 1615 (1987).
23. Weyama, N., Zaima, H., and Nakanuwa, A., *Chem. Lett.*, p. 1481 (1985).
24. Bishop, P. T., Dilworth, J. R., and Hughes, D. A., *J. Chem. Soc., Dalton Trans.*, p. 2535 (1988).
25. Bishop, P. T., Dilworth, J. R., and Zubieta, J. A., unpublished results (1982).
26. Dilworth, J. R., Hutchinson, J., and Zubieta, J. A., *J. Chem. Soc., Chem. Commun.*, p. 1034 (1983).
27. Blower, P. J., Dilworth, J. R., Hutchinson, J., Nicholson, T., and Zubieta, J. A., *J. Chem. Soc., Dalton Trans.*, p. 2639 (1985).
28. de Vries, N., Dewan, J. C., Jones, A. G., and Davison, A., *Inorg. Chem.* **27,** 1574 (1988).
29. Bishop, P. T., Dilworth, J. R., Nicholson, T., and Zubieta, J. A., *J. Chem. Soc., Dalton Trans.*, p. 385 (1991).
30. Bishop, P. T., Dilworth, J. R., Hutchinson, J., and Zubieta, J. A., *J. Chem. Soc., Dalton Trans.*, p. 967 (1986).
31. Bishop, P. T., Dilworth, J. R., Hutchinson, J., and Zubieta, J. A., *Inorg. Chim. Acta* **84,** L15–L16 (1984).
32. Murdzek, J. S., Blum, L., and Schrock, R. R., *Organometallics* **7,** 436 (1988).
33. Soong, S.-L., Chebolu, V., Koch, S. A., O'Sullivan, T., and Millar, M., *Inorg. Chem.* **25,** 4068 (1986).
34. Ellis, S. R., Collinson, D., and Garner, C. D., *J. Chem. Soc., Dalton Trans.*, p. 413 (1989).
35. Chisholm, M. H., Corning, J., and Huffman, J. C., *J. Am. Chem. Soc.* **105,** 5924 (1983).
36. Blower, P. J., Dilworth, J. R., and Zubieta, J. A., *Inorg. Chem.* **24,** 2866 (1985).
37. Burrow, T. E., Hills, A., Hughes, D. L., Lane, J. D., Morris, R. H., and Richards, R. L., *J. Chem. Soc., Dalton Trans.*, p. 1813 (1991).
38. Burrow, T. E., Hills, A., Hughes, D. L., Lane, J. D., Lazarowych, N. J., Maguire, M. J., Morris, R. H., and Richards, R. L., *J. Chem. Soc., Chem. Commun.*, p. 1757 (1990).
39. Fikar, R., Koch, S. A., and Millar, M., *Inorg. Chem.* **24,** 3311 (1985).
40. Power, P. P., and Shoner, S. C., *Angew. Chem., Int. Ed. Engl.*, **30,** 330 (1991).
41. Davison, A., de Vries, N., and Dewan, J. C., *Inorg. Chim. Acta* **120,** L15 (1986).
42. de Vries, N., Jones, A. G., and Davison, A., *Inorg. Chem.* **28,** 3728 (1989).
43. de Vries, N., Cook, J., Nicholson, T., and Jones, A. G., *Inorg. Chem.* **29,** 1062 (1990).
44. Hamor, T. A., Hussain, W., Jones, C. J., McCleverty, J. A., and Rothin, A. S., *Inorg. Chim. Acta* **146,** 181 (1988).
45. de Vries, N., Costello, C. E., Jones, A. G., and Davison, A., *Inorg.Chem.* **29,** 1348 (1990).

46. Blower, P. J., and Dilworth, J. R., *J. Chem. Soc., Dalton Trans.*, p. 1533 (1985).
47. Blower, P. J., and Dilworth, J. R., *J. Chem. Soc., Dalton Trans.*, p. 2305 (1985).
48. Bloch, E., Kang, H., Ofori-Okai, G., and Zubieta, J., *Inorg. Chim. Acta* **156,** 27 (1989).
49. Blower, P. J., and Dilworth, J. R., *Inorg. Chim. Acta* **90,** L27 (1984).
50. Dilworth, J. R., and Hu, J., unpublished results (1992).
51. Dilworth, J. R., Hu, J., Thompson, R., and Hughes, D. L., *J. Chem. Soc., Chem. Commun.*, p. 551 (1992).
52. Millar, M., Koch, S. A., and Fikar, R., *Inorg. Chim. Acta* **88,** 115 (1989).
53. Koch, S. A., Maelia, L. E., and Millar, M., *J. Am. Chem. Soc.*, **105,** 5944–5945 (1983).
54. Millar, M., Lee, J. F., Koch, S. A., and Fikar, R., *Inorg. Chem.* **21,** 4106–4108 (1982).
55. Gebhard, M. S., Deaton, J. C., Koch, S. A., Millar, M., and Solomon, E. I., *J. Am. Chem. Soc.* **112,** 2217 (1990).
56. Gebhard, M. S., Koch, S. A., Millar, M., Devlin, F. J., Stephens, P. J., and Solomon, E. I., *J. Am. Chem. Soc.* **113,** 1640 (1991).
57. Silver, A., Koch, S. A., and Millar, M., personal communication (1993).
58. Ueyama, N., Rerakawa, T., Sugawara, T., Fuji, M., and Nakamura, A., *Chem. Lett.*, p. 1287 (1984).
59. O'Sullivan, T., and Millar, M., *J. Am. Chem. Soc.* **107,** 4096 (1985).
60. Pickett, C. J., *J. Chem. Soc., Chem. Commun.*, p. 323 (1985).
61. Ueyama, N., Sugawara, T., Fuji, M., Nakamura, A., and Yasuoka, N., *Chem. Lett.*, p. 175 (1985).
62. Que, L., Bobrick, M. A., Ibers, J. A., and Holm, R.H., *J. Am. Chem. Soc.* **96,** 4168 (1973).
63. Papaefthymiou, V., Millar, M., and Munck, E., *Inorg. Chem.* **25,** 3010 (1986).
64. Ueyama, N., Ueno, S., Sugawara, T., Tatsumi, K., Nakamura, A., and Yasuoka,N., *J. Chem. Soc., Dalton Trans.*, p. 2723 (1991).
65. Koch, S. A., and Millar, M. M., *J. Am. Chem. Soc.* **105,** 3362 (1983).
66. Millar, M. M., O'Sullivan, T., and de Vries, N., *J. Am. Chem. Soc.* **107,** 3714 (1985).
67. Soong, S.-L., Hain, J. H., Jr., Millar, M., and Koch, S. A., *Organometallics* **7,** 556 (1988).
68. Catala, R. M., Cruz-Garritz, D., Sosa,P., Terreros,P., Torrens, H., Hills, A., Hughes, D. L., and Richards, R. L., *J. Organomet. Chem.* **359,** 219 (1989).
69. Hills, A., Hughes, D. L., Richards, R. L., Arroyo, M., Cruz-Garritz, D., and Torrens, H., *J. Chem. Soc., Dalton Trans.*, p. 1281 (1991).
70. Dilworth, J. R., Lu, S., Wu, Q., and Zheng, Y., *Inorg. Chim. Acta* **194,** 99 (1992).
71. Koch, S. A., Fikar, R., Millar, M., and O'Sullivan, T., *Inorg. Chem.* **23,** 122 (1984).
72. Fikar, R., Koch, S. A., and Millar, M., *Inorg.Chem.* **24,** 3311 (1985).
73. Corwin, D. T., Jr., Fikar, R., and Koch, S. A., *Inorg. Chem.* **26,** 3080–3082 (1987).
74. Bishop, P. T., Dilworth, J. R., Hutchinson, J., and Zubieta, J. A., *J. Chem. Soc., Chem. Commun.*, p. 1952 (1982).
75. Blower, P. J., Dilworth, J. R., Hutchinson, J., and Zubieta, J. A., *J. Chem. Soc., Dalton Trans.*, p. 1339 (1986).
76. Bishop, P. T., Dilworth, J. R., Nicholson, T., and Zubieta, J. A., *J. Chem. Soc., Chem. Commun.*, pp. 1123–1125 (1986).
77. Garcia, J. J., Torrens, H., Adams, H., Bailey, N. A., and Maitlis, *J. Chem. Soc., Chem. Commun.*, p. 74 (1991).
78. Bonnett, J. J., Thorez, A., Mansonnat, A., Galy, J., and Poilblanc, R., *J. Am. Chem. Soc.* **101,** 5940 (1979).
79. Pinillos, M. T., Elduque, A., Oro, L. A., Lahoz, F., Bonati, F., Tiripicchio, A., and Tiripicchio-Camellini, M., *J. Chem. Soc., Dalton Trans.*, p. 989 (1990).

80. Dilworth, J. R., and Zheng, Y., unpublished results.
81. Eidsness, M. K., Sullivan, R. J., and Scott, R. A., *in* "The Bioinorganic Chemistry of Nickel (J. R. Lancaster, ed.), Chapter 4. VCH Publishers, New York, 1988.
82. Baidya, N., Olmstead, M., and Mascharak, P. K., *Inorg. Chem.* **30,** 929 (1991).
83. Uson, R., Fornies, J., Uson, M. A., and Apaolaza, J. A., *Inorg. Chim. Acta* **187,** 175 (1991).
84. Coucouvanis, D., Murphy, C. N., and Kanodia, S. K., *Inorg. Chem.* **19,** 2993 (1980).
85. Dance, I. G., *Aust. J. Chem.* **31,** 2195 (1978).
86. Dance, I. G., and Calabrese, J. C., *Inorg. Chim. Acta* **19,** L41 (1976).
87. Bloch, E., Kang, H., Ofori-Okai, G., and Zubieta, J., *Inorg. Chim. Acta* **29,** 147 (1990).
88. Yang, Q., Tang, K., Liao, Y., Han, Y., Chen, Z., and Tang, Y., *J. Chem. Soc., Chem. Commun.*, p. 1076 (1987).
89. Schröter-Schmid, I., and Strähle, J., *Z. Naturforsch. B: Chem. Sci.* **45B,** 1537–1542 (1990).
90. Bloch, E., Gernon, M., Kang, H., Liu, S., and Zubieta, J., *J. Chem. Soc., Chem. Commun.*, p. 1031 (1988).
91. Nicholson, J. R., Abrams, I. L., Clegg, W., and Garner, C. D., *Inorg. Chem.* **24,** 1092 (1985).
92. Schröter, I., and Strähle, J., *Chem. Ber.* **124,** 2161 (1991).
93. Fairall, L., Klug, A., and Rhodes, D., *J. Mol. Biol.* **192,** 577 (1986).
94. Brown, R. S., and Argos, P., *Nature (London)* **324,** 215 (1986).
95. Berg, J. M., *Science* **232,** 485 (1986).
96. Corwin, D. T., Jr., Gruff, E. S., and Koch, S. A., *J. Chem. Soc., Chem. Commun.*, p. 966 (1987).
97. Corwin, D. T., Jr., and Koch, S. A., *Inorg. Chem.* **27,** 493 (1988).
98. Power, P. P., Corwin, D. T., Jr., and Shoner, S. C., *Angew. Chem., Int. Ed. Engl.* **29,** 1403 (1990).
99. Gruff, E. S., and Koch, S. A., *J. Am. Chem. Soc.* **111,** 8762 (1989).
100. Cotton, F. A., and Wilkinson, G., "Advanced Inorganic Chemistry." Wiley, New York, 1988.
101. Corwin, D. T., Jr., Gruff, E. S., and Koch, S. A., *Inorg. Chim. Acta* **151,** 5 (1988).
102. Gruff, E. S., and Koch, S. A., *J. Am. Chem. Soc.* **112,** 1245 (1990).
103. Santos, R. A., Gruff, E. S., Koch, S. A., and Harbison, G. S., *J. Am. Chem. Soc.*, **113,** 469–475 (1991).
104. Alsina, T., Clegg, W., Fraser, K. A., and Sola, J., *J. Chem. Soc., Chem. Commun.*, p. 1010 (1992).
105. Bochmann, M., Webb, K., Harman, M., and Hursthouse, M. B., *Angew. Chem., Int. Ed. Engl.* **102,** 638 (1990).
106. Tang, K., Li, A., Jin, X., and Tang, Y., *J. Chem. Soc., Chem. Commun.*, p. 1590 (1991).
107. Cetinkaya, B., Gumrukcu, I., Lappert, M., Atwood, J. L., and Shakir, R., *J. Am. Chem. Soc.* **102,** 2086 (1980).
108. Aslam, M., Bartlett, R. A., Bloch, E., Olmstead, M. M., Power, P.P., and Sigel, G. A., *J. Chem. Soc., Chem. Commun.*, p. 1674 (1985).
109. Ruhlandt-Senge, K., and Power, P. P., *Inorg. Chem.* **30,** 2633 (1991).
110. Maelia, L. E., and Koch, S. A., *Inorg. Chem.* **25,** 1896 (1986).
111. Hitchcock, P. B., Lappert, M. F., Samways, B. J., and Weinberg, E. L., *J. Chem. Soc., Chem. Commun.*, p. 1492 (1983).
112. Burrow, T. E., Lough, A. J., Morris, R. H., Hills, A., Hughes, D. L., Lane, J. D., and Richards, R. L., *J. Chem. Soc., Dalton Trans.*, p. 2519 (1991).

APPENDIX: SUMMARY TABLE OF STERICALLY HINDERED THIOLATE COMPLEXES

| Complex | Structure | Reference |
|---|---|---|
| $[Ti(TIPT)]_4^{-1}$ | Tetrahedral | *13* |
| $[Ti(TEMT)_4]$ | — | *12* |
| $[Zr(TEMT)_4]$ | — | *12* |
| $[Zr_3S(SBu^t)_{10}]$ | $Zr_3(\mu\text{-}SBu^t)_3$ core with capping $SBu^t$ and S ligands | *15b* |
| $[Zr_3S_2(BH_4)_4(THF)_2]$ | $Zr_3(\mu_3\text{-}S)(\mu\text{-}S)(\mu\text{-}SBu^t)_2$ core with terminal bi- and tridentate $BH_4$ ligands | *15c* |
| $[V(SR)_4]^{0,1-}$ | Tetrahedral | *16* |
| $[V(TIPT)_3(THF)_2]$ | Trigonal bipyramidal | *17* |
| $[Ta(TEMT)_5]$ | Trigonal bipyramidal | *12* |
| $[V(Bu^tN)(SBu^t)_3]$ | Tetrahedral | *18* |
| $[V(Bu^tN)(SBu^t)_2Cl]$ | — | *18* |
| $[V(Bu^tN)(SBu^t)Cl_2]$ | — | *18* |
| $[V(Bu^tN)(SSiPh_3)_3]$ | — | *18* |
| $[\{V(Bu^tN)(SSiPh_3)_2\}_2O]$ | Dimeric, oxo bridge. | *18* |
| $[Mo(SBu^t)_4]$ | Tetrahedral | *20* |
| $[Mo(TIPT)_4]$ | Tetrahedral | *14, 23* |
| $[Mo(TEMT)_4]$ | — | *14* |
| $[MoCl(TIPT)_4]$ | — | *14* |
| $[Mo(TIPT)_4L]$ (L = alkene, MeCN, CO) | Trigonal bipyramidal | *22, 24* |
| $[Mo(=N—N=CPh_2)(TIPT)_4]$ | — | *22* |
| $[Mo(=N—NMePh)(TIPT)_4]$ | — | *25* |
| $[Mo(CO)_2(TIPT)_3]^{-1}$ (also for DIPT, DMT, PFT) | Trigonal bipyramidal, axial CO | *26* |
| $[Mo(TIPT)_3(CO)L]^-$ (L = $PMe_2Ph$, $CNBu^t$, $NCBu^t$) | — | *27* |
| $[Mo(TIPT)_2(CO)_2(PMe_2Ph)_2]$ | — | *112* |
| $[Mo(NNPh)(MeCN)(TIPT)_3]$ | — | *27* |
| $[Mo(TIPT)_3(CO)_3]^-$ | — | *27* |
| $[Mo(SC_6H_3\text{-}2\text{-}Ph\text{-}6\text{-}(\eta^6\text{-}C_6H_5)](DPT)(CO)]$ | "Three-legged piano stool," with arene substituent $\eta^6$-bonded to Mo | *29* |
| $[Mo(DPT)_2(CO)_2L]$ (L = bipy, phen, or CO) | Octahedral (L = bipy) | *29* |
| $[Mo(TIPT)_3(NH_3)(NO)]$ | Trigonal bipyramidal, apical NO and $NH_3$ | *30* |
| $[Mo(\equiv CBu^t)(TMT)_3]$ (also for TIPT) | — | *32* |
| $[MoO(TIPT)_4]^{1-}$ (also for TMT) | Square pyramidal, apical oxo-group | *33, 34* |
| $[MoO(PFTP)_4]^{1-}$ | — | *34* |
| $[MoO(PFTP)_4]^{2-}$ | — | *34* |
| $[Mo_2(TIPT)_6]$ (also for TMT) | Dimeric with M—M triple bond | *35, 36* |
| $[MoH(TIPT)_3(PMe_2Ph)_2]$ (also for TMT) | Distorted trigonal bipyramidal | *37* |

(*continued*)

APPENDIX: (*Continued*)

| Complex | Structure | Reference |
|---|---|---|
| $[MoH(TIPT)_3(PMePh_2)]$ (also for TMT, $PEt_2Ph$) | — | *38* |
| $[\{Mo(TIPT)(OMe)(PMePh_2)(\mu\text{-}S)\}_2]$ | Dimeric with $Mo(\mu\text{-}S_2)Mo$ core | *38* |
| $[W(SBu^t)_4]$ | Tetrahedral | *22* |
| $[W(\equiv CBu^t)(TIPT)_3]$ (also for TMT) | — | *32* |
| $[WO(TIPT)]_4^-$ | Square pyramidal with axial oxo-group | *33, 34* |
| $[WH(TIPT)_3(PMe_2Ph)_2]$ (also for TMT) | — | *37* |
| $[Mn(TIPT)_4]^-$ | Tetrahedral | *39* |
| $[\{Mn(TBT)_2\}_2]$ | Trigonal planar, with bridging thiolate groups | *40* |
| $[Tc(TEMT)_3(MeCN)_2]$ (also for TIPT) | Trigonal bipyramidal, axial MeCN ligands | *28, 41* |
| $[Tc(TEMT)_3L_2]$ (L = CO, *i*-PrCN, Py) (also for TIPT) | — | *28* |
| $[Tc(TEMT)_3(CO)L]$ (L = Py, MeCN) (also for TIPT) | — | *28* |
| $[TcO(TIPT)_3(Py)]$ (also for TEMT) | Square pyramidal | 42 |
| $[Tc(NO)(Cl)(TEMT)_3]$ | Trigonal bipyramidal with axial Cl and NO | *43* |
| $[TcO(TEMT)_4]^-$ (also for DIPT, TIPT) | Square pyramidal with axial oxo-ligand | *28, 41, 44* |
| *trans*-$[TcN(TEMT)_2(NHC(NMe_2)_2)_2]$ | Square pyramidal with apical nitrido-ligand | *45* |
| *trans*-$[TcN(TEMT)_2(Py)_2]$ | — | *45* |
| $[Re(TIPT)_4(NO)]$ | Trigonal bipyramidal | *46* |
| $[Re(TIPT)_3(NCMe)_2]$ (also for DIPT, TMT) | — | *47* |
| $[Re(TIPT)_3(MeCN)(PPh_3)]$ | — | *47* |
| $[Re(STP)\{NC(STP)CH_3\}_2(PPh_3)_2]$ | Trigonal bipyramidal | *48* |
| $[ReO(TIPT)_4]^{1-}$ (also for DIPT, TMT, TEMT, DPT) | Square pyramidal with apical oxo-group | *49* |
| $[ReN(TIPT)_4]^{n-}$ ($n$ = 1,2) | — | *47* |
| $[Ph_4P][Re(NR')(TIPT)_4]$ (R'=Ph, $C_6H_4Me$, or $C_6H_4OMe$) | — | *47* |
| $[Re(DMT)_3(PPh_3)]$ | Trigonal bipyramidal with axial agostic interaction with Me hydrogen | *50* |
| $[Re(TIPT)_3(N_2)(PPh_3)]$ | Trigonal bipyramidal with axial $N_2$ and $PPh_3$ | *51* |
| $[Fe(TMET)_4]^-$ | Tetrahedral | *52, 54* |
| $[Fe(TIPT)_4]^-$ (also for DMT) | Tetrahedral | *52, 54* |
| $[Fe_4S_4(SBu^t)_4]^{2-}$ | Cubane-like $Fe_4S_4$ core | *58* |
| $[Fe_4S_4(TIPT)_4]^{2-}$ (also for TMT) | Cubane-like $Fe_4S_4$ core | *58, 59, 61* |
| $[Fe_4S_4(TIPT)_4]^{2-}$ (also for TMT) | Cubane-like $Fe_4S_4$ core | *58, 59, 61* |

(*continued*)

APPENDIX: (*Continued*)

| Complex | Structure | Reference |
|---|---|---|
| $[NEt_4][Fe_2S_2(TMT)_4]$ | Dimeric with terminal TMT and planar $Fe_2S_2$ core | *64* |
| $[\{Fe(TBT)_2\}_2]$ | Dimeric with bridging TBT and trigonal planar Fe | *40* |
| $[Ru(TIPT)_4(MeCN)]$ (also for TEMT, Os) | Trigonal bipyramidal with axial MeCN | *65* |
| $[Ru(TIPT)_4(CO)]$ (also for TEMT, Os) | Trigonal bipyramidal with axial CO | *66* |
| $[Ru(TIPT)_4(NO)]^-$ (also for DMT, TIPT) | Trigonal bipyramidal with axial NO | *67* |
| $[Ru(TIPT)_4L]$ (L = MeOH, DMSO) | — | *67* |
| $[Ru(TIPT)_4]$ | Trigonal bipyramidal with agostic interaction with methine H in axial site | *67* |
| $[Ru_2(TEMT)_7(NO)_2]$ | Octahedral with three bridging TEMT ligands, two with agostic interactions via Me groups | *67* |
| $[Ru(PFTP)_3(PMe_2Ph)_2]$ | Octahedral coordination with the F group bonded to Ru | *68* |
| $[Ru(PFTB)_2(PPh_3)_2]$ | Octahedral coordination with $\sigma$-bonded phosphine phenyls | *68* |
| $[Os(PFTP)_3(PMe_2Ph)_2]$ | Trigonal bipyramidal with axial Cl and P ligands | *69* |
| $[Co(TEMT)_3(NCCH_3)]^-$ | Tetrahedral | *71* |
| $[Co(TEMT)_4]^{2-}$ | — | *71* |
| $[Co(TIPT)_4]^-$ | Square planar | *72* |
| $[Co(TIPT)_2L_2]$ (L = Py, MeCN, imidazole) | Tetrahedral | *73* |
| $[Co(TIPT)_2(bipy)(NCCH_3)]$ | Trigonal bipyramidal | *73* |
| $[Co(DIPT)_2(2,9\text{-}Me_2Phen)]$ | Tetrahedral | *73* |
| $[Co(TEMT)_2(bipy)]_2$ | Octahedral | *73* |
| $[\{Co(TBT)_2\}_2]$ | Dimeric with bridging TBT, trigonal planar Co | *40* |
| $[Rh_2\{\mu\text{-}SC_6H_3\text{-}2\text{-}(C_6H_4)\text{-}6\text{-}Ph\}_2(DPT)_2(NCCH_3)_2]$ | Dimeric with bridging DPT, also $\sigma$-bonded via 2-Ph | *29* |
| $[Rh_2\{\mu\text{-}SC_6H_2Pr^i_2\text{-}4,6,2\text{-}(\eta^2\text{-}MeC{=}CH_2)\}_2\{TIPT\}_2(NCCH_3)]$ | Asymmetric binuclear structure with bridging TIPT with the $Pr^i$-group dehydrogenated to give olefin | *76* |
| $[Rh_2(PFTP)_2(CO)_4]$ | Dimeric with bridging PFTP ligands | *77* |
| $[Ir_2(SBu^t)_2(CO)_2(PR_3)_2]$ | Dimeric with bridging $SBu^t$ ligands | *78* |
| $[IrH(TPSTP)_2(PMePh_2)_3]$ | Octahedral coordination with H *trans* to S | *80* |

(*continued*)

APPENDIX: (*Continued*)

| Complex | Structure | Reference |
|---|---|---|
| $[Ni(terpy)(TIPT)_2]$ | Trigonal bipyramidal | *82* |
| $[Pd(PFTP)_4]^{2-}$ (also for Pt) | — | *83* |
| $[Cu(TEMT)_2]^-$ | Linear | *71* |
| $[Cu_4(BSTP)_4]$ | Planar 8-membered ring | *87* |
| $[Cu_8(TIPT)_8]$ (isomer 1) | Twisted 16-membered ring | *88* |
| $[Cu_8(TIPT)_8]$ (isomer 2) | Folded 16-membered ring | *89* |
| $[Cu_4(TIPT)_4]$ | Eight-membered ring | *89* |
| $[Cu_{12}(STP)_{12}]$ | Paddle-wheel-like cluster structure | *87, 90* |
| $[Ag_3\{SC(SiPhMe_2)_3\}_3]$ | Six-membered ring | *8* |
| $[Ag_4\{SC(SiMe_3)_3\}_4]$ | Eight-membered ring | *8* |
| $[\{Ag_4(SCH(SiMe_3)_2)_4\}_2]$ | Two 8-membered rings linked by Ag—S interactions | *8* |
| $[\{Ag_4(STP)_4\}_2]$ | Two 8-membered rings linked by Ag—S interactions | *11* |
| $[Au_6(TIPT)_6]$ | Twelve-membered ring in chair conformation | *92* |
| $[Au(TIPT)_2]^-$ | Linear | *92* |
| $[Cd(TIPT)_2(1\text{-}CH_3\text{-}imid)_2]$ | Tetrahedral | *96* |
| $[Zn(TIPT)_2(bipy)]$ | Tetrahedral | *97* |
| $[Zn(TEMT)_2(1\text{-}CH_3\text{-}imid)_2]$ | Tetrahedral | *97* |
| $[Zn(TBT)_2(OEt_2)]$ | T-shaped | *98* |
| $[Zn(TEMT)_3]^-$ | Y-shaped | *99* |
| $[Pr_4^nN][Zn(TEMT)_3(1\text{-Me-imid})]$ | Tetrahedral | *99, 101* |
| $[Zn(TEMT)_4]^{2-}$ | Tetrahedral | *99* |
| $[Pr_4^nN]_2[Cd_2(TEMT)_6]$ | – | *99* |
| $[PPh_4][Cd(TIPT)_3]$ | $C_{3h}$ symmetry | *102* |
| $[Bu_4^nN][Cd(TIPT)_3]$ | Y-shaped | *103* |
| $[Cd(TBT)_3]^-$ | — | *103* |
| $[Hg(TIPT)_3]^-$ (also for TEMT) | Y-shaped | *102* |
| $[Hg_7(SC_6H_{11})_{12}Br_2]$ | Complex cluster structure with central octahedrally coordinated Br | *104* |
| $[\{Cd(TBT)_2\}_2]$ | Dimeric structure with bridging TBT and trigonal planar Cd | *105* |
| $[Cd_3(TIPT)_7]^-$ | Defective cubane structure with one missing vertex | *106* |
| $[Li(THF)_3(TBT)]$ | Tetrahedral | *13* |
| $[Ga(TIPT)_4]^-$ (also for TEMT) | — | *110* |
| $[Al(TBT)_3]$ | Trigonal planar | *109* |
| $[Ga(TBT)_3]$ | Trigonal planar | *109* |
| $[Ge(TBT)_2]$ (also for Sn) | V-shaped | *109* |
| $[Pb(TIPT)_2]$ | — | *111* |
| $[Sn_3(TIPT)_6]$ (also for Ge and Pb) | Linear trimer with bridging TIPT groups | *111* |